UNIVERSITA' DI NAPOLI FEDERICO II

DOTTORATO DI RICERCA
BIOCHIMICA E BIOLOGIA CELLULARE E MOLECOLARE
XXVI CICLO

7-DEHYDROCHOLESTEROL AND ITS OXIDATIVE COMPOUNDS: STABILITY STUDY AND THEIR EFFECTS ON MELANOMA CELL LINES

Monica Gelzo

Tutor
Prof. Gaetano Corso

Coordinator
Prof. Paolo Arcari

Co-Tutor
Prof. Maria Rosaria Ruocco

Academic Year 2012/2013

La scienza è fatta di dati,
come una casa di pietre.
Ma un ammasso di dati non è scienza
più di quanto un mucchio di pietre sia una casa.

(Henri Poincaré, La scienza e l'ipotesi, 1902)

Ringraziamenti e Dediche

Voglio ringraziare tutte le persone che, in diversa misura, hanno contribuito alla mia formazione scientifica. Ringrazio, il Prof. Gaetano Corso per avermi guidato sempre, e per aver creduto nelle mie potenzialità scientifiche. La Prof.ssa Maria Rosaria Ruocco per i preziosi insegnamenti e per avermi sempre supportata ed incoraggiata. Il Prof. Antonio Dello Russo per la fiducia e per i diversi incarichi che mi ha affidato.

Inoltre, voglio esprimere la mia gratitudine ai Proff. Paolo Arcari, Emmanuele De Vendittis, Mariorosario Masullo, ed Alessandro Arcucci per la loro gentilissima ed immancabile disponibilità. Ringrazio inoltre Francesco e Giusy per la loro importante collaborazione a questo lavoro di tesi.

Un grazie di cuore ad Anna per tutto l'affetto e per essermi stata vicina in ogni momento. Come non ringraziare Nicola, Doriana e Valentina per tutti i saggi consigli e l'amicizia mostrata. Inoltre, ringrazio tutti i ricercatori, gli amici e gli specializzandi del VI piano della Torre Biologica per avermi fatto sentire parte di una grande famiglia.

Un grazie speciale va ai miei genitori, Alfredo e Giovanna, e mio marito, Salvatore, per il grande sostegno ed in particolare per essere stati sempre presenti ed amorevoli.

Grazie,

Monica

Riassunto

Il 7-deidrocolesterolo (7-DHC), il precursore biosintetico del colesterolo, è una molecola che si modifica facilmente producendo composti ossidati. Prove *in vitro* hanno dimostrato che l'instabilità del 7-DHC in soluzione e nei liposomi è dovuta alla sua suscettibilità alla perossidazione. Inoltre, il 7-DHC è convertito nella vitamina D3 mediante la sintesi foto-indotta che avviene nella pelle. Il 7-DHC che è presente a concentrazioni relativamente elevate nella pelle, è esposto all'attacco dei radicali esogeni e dall'ossigeno. Recentemente è stato riportato che i composti ossidati del 7-DHC possono esercitare effetti deleteri sulla funzionalità e sulla vitalità cellulare.

Le radiazioni ultraviolette rappresentano la causa principale dei tumori della pelle ed il melanoma ne è la forma più grave. La diagnosi tardiva del melanoma è particolarmente infausta in quanto tale neoplasia nello stadio avanzato è refrattario alle terapie.

In questo studio abbiamo valutato l'effetto del 7-DHC "come tale" (non modificato) su linee cellulari di melanoma ed a tale scopo è stata posta molta attenzione a minimizzare le modifiche del 7-DHC. Abbiamo quindi valutato la stabilità del 7-DHC nella sospensione del veicolo utilizzata per il trasferimento del 7-DHC dal mezzo di coltura all'interno delle cellule. Inoltre, abbiamo determinato i livelli intracellulari del 7-DHC e dei suoi composti derivati dopo diversi tempi di trattamento.

Lo studio di stabilità nel tempo non ha mostrato variazioni significative dei livelli del 7-DHC nella sospensione conservata per 90 giorni a 4 °C. Abbiamo osservato che da 12 a 72 ore di trattamento l'82-86% di 7-DHC entrava nelle cellule ed i livelli dei composti derivati dal 7-DHC non erano significativi. Allo stesso tempo, la produzione di ROS aumentava in modo significativo già dopo 2 ore. Dopo 24 ore e fino a 72 ore, le cellule di melanoma trattate con 7-DHC hanno mostrato una riduzione della crescita e della vitalità cellulare. L'effetto citotossico del 7-DHC era associato ad aumento dei livelli di Bax, diminuzione del rapporto Bcl-2/Bax, riduzione del potenziale di membrana mitocondriale, aumento dei livelli del fattore che induce apoptosi (AIF), a nessuna variazione dell'attività della caspasi-3 così come all'assenza della forma inattiva di PARP-1. Tali risultati contribuiscono a spiegare il meccanismo attraverso il quale il 7-DHC esercita il suo effetto citotossico.

Nel complesso i risultati ottenuti nel corso di questo lavoro indicano che il 7-DHC esercita un effetto citotossico su linee cellulari di melanoma, probabilmente attraverso un processo pro-apoptotico caspasi indipendente e allargano le conoscenze sulle prospettive terapeutiche del cancro.

Summary

The 7-dehydrocholesterol (7-DHC), the precursor of cholesterol biosynthesis, is highly reactive and easily modifiable to produce 7-DHC oxidative compounds. Evidences *in vitro* demonstrated that the instability of 7-DHC in solution and in liposomes is due to its susceptibility to peroxidation. In addition, 7-DHC is also converted in vitamin D3 by photo-induced synthesis which occurs in the skin. 7-DHC is present at relatively high concentrations in skin where it is exposed to exogenous radical sources and oxygen. Recently, it has been reported that 7-DHC oxidative compounds can have deleterious effects on cellular functionality and viability.

Ultraviolet radiation is the main cause of skin cancers, and melanoma is the most serious form of tumor. Today, there is no therapy for advanced-stage melanoma and its metastasis due to their high resistance to various anticancer therapies.

In this study, we evaluated the effect on melanoma cell lines of 7-DHC as such, and for this aim much care to minimize 7-DHC modifications was used. Therefore, we evaluated the 7-DHC stability in the vehicle suspension used to transfer this compound from the culture medium into the cells. We also measured the intracellular levels of 7-DHC and its oxidative compounds after different treatment times.

The stability study showed no significant changes of 7-DHC levels from baseline values in the suspension up to 90 days of storage at 4 °C.

We found that from 12 to 72 hours of treatment 82-86% of 7-DHC entered the cells, and the levels of 7-DHC-derived compounds were not significant. Simultaneously, ROS production was significantly increased already after 2 hours. After 24 hours and up to 72 hours, 7-DHC treated melanoma cells showed a reduction of cell growth and viability. The cytotoxic effect of 7-DHC was associated with the increase of Bax levels, the decrease of Bcl-2/Bax ratio, the reduction of mitochondrial membrane potential, the increase of apoptosis inducing factor (AIF) levels, the unchanged caspase-3 activity, and uncleavage of PARP-1. These findings could explain the mechanism through which 7-DHC exerts its cytotoxic effect.

The results of this study show that the 7-DHC has a potential pro-apoptotic on melanoma cell lines, shed light on the possible mechanisms through which this molecule exerts its cytotoxic effects and, at same time, may give new insights in the therapeutic perspective of cancer.

Index

List of Tables

List of Figures

1. Introduction

1.1 7-Dehydrocholesterol and its oxidative compounds

The 7-dehydrocholesterol (7-DHC) is the direct precursor of cholesterol and contains an unsaturated B ring with two double bonds in position 5 and 7, which is reduced by delta7-sterol reductase to produce cholesterol [1,2]. Inherited defects in this enzyme reduce or abolish the transformation of 7-DHC to cholesterol with accumulation of 7-DHC and its isomer 8-dehydrocholesterol (8-DHC), in blood and tissues, well described in the Smith Lemli Opitz syndrome (SLOS; MIM 270400). Patients affected by this disorder have multiple morphogenic and congenital anomalies including internal organ, skeletal and/or skin abnormalities [3]. Clinical severity correlates negatively with the cholesterol concentration, and positively with the 7-DHC concentration and the sum of dehydrocholesterols (DHC) [4].

In a previous study we described our experience in laboratory diagnosis of SLOS and other defects of cholesterol biosynthesis analyzing the sterol profiles in plasma and erythrocyte membranes by gas chromatography paired to mass spectrometry (GC-MS). In particular, we measured cholesterol and its precursors, such as 7-DHC, desmosterol, 8-DHC, lathosterol, and exogenous sterols, such as campesterol, stigmasterol, and sitosterol. Furthermore, in order to ascertain the stability of the DHC, we evaluated storage effects on cholesterol and DHC concentrations in plasma and erythrocyte membranes from SLOS and unaffected subjects. We observed that the oxidation rate of DHC in erythrocyte membranes was at least 2-fold higher than that in plasma [5]. From our experience and according to others, DHC in plasma are relatively stable, but substantial autoxidation would be expected for DHC in plasma and whole blood adsorbed onto filter paper and exposed to air for long periods of time [6,7]. Based on these results, we have recently developed a procedure to stabilize DHC in dried spot of blood from patients with SLOS using a filter-paper treated with butylated hydroxytoluene as antioxidant [8,9].

Autoxidation of lipids, such as polyunsaturated fatty acids (PUFAs) and sterols, has attracted research attention over the last few decades due to its involvement in the patho-physiology of common diseases. Lipids are extremely prone to react with molecular oxygen and cholesterol free radical oxidation has been studied in great detail because some of its peroxide products have potent biological activities [10,11].

Experimental evidences *in vitro* demonstrated that the instability of 7-

DHC in solution and in liposomes is due to its susceptibility to peroxidation, which is at least 10-fold more reactive than arachidonic acid, and at least 200-fold more reactive than cholesterol [12]. Recently, over a dozen oxysterols were isolated and characterized from free radical chain oxidation of 7-DHC [13].

In addition, 7-DHC is also known as pro-vitamin D, the precursor of vitamin D3 (cholecalciferol). The photochemical isomerization of 7-DHC after absorption of UV-B photons to the pre-vitamin D3 intermediate, followed by its slow isomerization to three main products including vitamin D3, tachysterol, and lumisterol (L3), represents the most fundamental reactions in the photobiology of the skin [14]. Increasing evidences indicate that the UV-B-mediated cutaneous photosynthesis of 1,25-dihydroxyvitamin D3 ($1,25(OH)_2D3$), the active form of vitamin D, represents an evolutionary highly conserved endocrine system that protects the skin against environmental hazards, including UV [15-19].

Human skin is a fundamental body organ involved in the internal homeostasis by separating the external from the internal environments, and through its immune and neuroendocrine activities [20]. The skin is an organ frequently exposed to sunlight and it is well known that ultraviolet radiation is the main cause of skin cell damage that ultimately leads to skin cancer. Indeed, the melanocytes, pigment-producing cells in the skin, can transform into melanoma cells, the most serious form of skin cancer. When detected early, melanoma is considered curable, but when detected at later stages it is one of the most lethal malignancies. Surgery is standard treatment for localized melanoma; unfortunately, there is no standard therapy for advanced-stage melanoma. Metastatic melanoma disseminates widely and it frequently involves sites that are not commonly affected in other cancers, such as the gastrointestinal tract and skin. Systemic therapies are known to be ineffective, because of the high resistance of melanoma cells to various anticancer therapies [21].

1.2 Effects of 7-DHC and its derivative compounds

7-DHC is present at relatively high concentrations in skin where it is exposed to exogenous radical sources and oxygen. The intracellular levels of 7-DHC could have deleterious effects on cellular functionality, either through altering the composition of the membranes or causing an intracellular redox imbalance. In addition, 7-DHC oxidative derivatives, oxysterols, can affect the cellular viability inducing cytotoxicity [22], the immune response [23], and influencing the regulation of cholesterol homeostasis [24,25]. However, the study of the effects on cancer cells,

stimulated by the addition of 7-DHC alone to culture medium is rarely reported in the literature.
In keratinocytes, when cholesterol is partially replaced by 7-DHC, a rapid increase of intracellular ROS levels has been observed [26]. Since 7-DHC is not a chromophore, at present, it is not clear how the 7-DHC causes the redox state alterations responsible of UV-A skin photosensibility.
In the membranes cholesterol can be displaced by 7-DHC and contributing to affect lipid raft architecture. In fact, it has been suggested that the alteration of signaling pathways, triggered by the modification in the lipid raft composition in a keratinocyte model, is associated to an increase of UV-A-induced ROS formation [15]. Therefore, the high levels of 7-DHC can provoke cellular changes through a two-step mechanism: i) displacing the cholesterol, 7-DHC alters the composition of cellular membranes, ii) the high reactivity of 7-DHC makes this molecule easily modifiable producing several 7-DHC-derived compounds. Recently, in normal cells and in a SLOS cell model it was observed that 7-DHC-derived oxysterols altered the expression of molecules involved in the intracellular signaling, lipid biosynthesis, and vesicular transport [27,28].

1.3 Scientific hypothesis and aim of the work

In this study we have hypothesized that the evaluation of cytotoxic potential of 7-DHC could be of interest in a neoplastic context.
We have treated melanoma cell lines with 7-DHC at concentrations likely to that detected in plasma of SLOS patients with a mild phenotype.
In order to understand the direct effects of 7-DHC, we evaluated the 7-DHC stability in the vehicle suspension used to transfer the 7-DHC from the culture medium into the cells.
We have studied the cytotoxic effect of 7-DHC on melanoma cells, evaluating its pro-apoptotic potential, and the molecular processes that regulate the cell death up to 3 days of treatment.
We have measured the intracellular levels of 7-DHC and its oxidized derivatives after different treatment times.

2. Materials and Methods

2.1 Materials

The analytical solvents of HPLC grade, including methanol, dichloromethane, n-hexane, ethanol, and pyridine were purchased from Carlo Erba Reagenti (Milano, Italy). Ursodeoxycholic acid, sterol standards, oxysterols, butylated hydroxytoluene (BHT), and N,O-bis(trimethylsilyl)trifluoroacetamide (BSTFA) were purchased from Sigma–Aldrich Ltd. (St. Louis, MO, USA). Sodium ursodeoxycholate (NaUDC) was prepared by neutralizing ursodeoxycholic acid dissolved in 95% ethanol with a stoichiometric amount of aqueous sodium hydroxide solution [29], the solution was dried under nitrogen, and dissolved in methanol to provide a solution of 12.4 g/L. BHT was dissolved in ethanol to provide a stock solution of 60 g/L. Stock solutions of sterol standards were prepared in chloroform/methanol (2:1, v/v) to provide solutions of 0.4 g/L for 5α-cholestane (internal standard), 1 g/L for cholesterol, and 3.85 g/L for 7-DHC. Stock solutions of oxysterols (cholesterol 5β,6β-epoxide, 25-hydroxy-cholesterol, and 7-keto-cholesterol) were prepared in methanol to provide solutions of 1 g/L. All solutions were stored at -20 °C. Dulbecco's modified eagle's medium (DMEM), Roswell Park Memorial Institute (RPMI) 1640 medium, fetal bovine serum (FBS), L-glutamine, penicillin G, streptomycin, trypsin were purchased from Lonza (Milano, Italy). Annexin V-FITC was purchased from BD Pharmigen (Milano, Italy). Propidium iodide (PI), dichlorofluorescein diacetate (DCFH-DA), Rhodamine 123 (R123), apocynin, N-acetyl-L-cysteine (NAC) were purchased from Sigma-Aldrich Ltd. A protease inhibitor cocktail was obtained from Roche Diagnostics S.p.A. (Monza, Italy). Caspase-3 fluorometric assay kit was purchased from BioVision (Milpitas, CA, USA), and EnzyChrome GSH/GSSG assay kit was purchased from BioAssay Systems (Hayward, CA, USA). Rabbit monoclonal antibody against AIF was from Abcam (Cambridge, UK); rabbit monoclonal antibody against GAPDH was obtained from Cell Signalling (Boston, MA, USA); mouse monoclonal antibody against Bcl-2, rabbit polyclonal antibody against Bax, goat polyclonal antibody against β-actin, rabbit polyclonal antibody against poly(ADP-ribose) polymerase 1 (PARP-1), and each secondary antibody conjugated to horseradish peroxidase were obtained from Santa Cruz Biotechnology (Heidelberg, Germany). All other chemicals were of analytical grade and were purchased from Sigma-Aldrich Ltd.

2.2 Preparation of 7-DHC-enriched media

Two suspensions containing 12.4 g/L NaUDC enriched with 3.85 g/L 7-DHC and NaUDC alone (vehicle) were prepared by a modified dispersion method [30,31]. Briefly, 2 mL of NaUDC alone or a mix of 2 mL of 7-DHC and 2 mL of NaUDC were dried under nitrogen and dissolved with 2 mL of phosphate buffer (50 mM, pH 7.4). The suspensions were sterilized by autoclaving (121 °C for 20 min), and then mixed vigorously on a vortex, incubated at 65 °C for 15 min and sonicated for 20 min (three times). These suspensions were diluted 1:10 with FBS and, after incubation at 37° C for 1.5 hours alternating with vortex agitation, the 7-DHC-enriched FBS and the 7-DHC-free FBS were diluted ten fold with medium to obtain final concentrations of 38.5 μg/mL for 7-DHC and 124 μg/mL for NaUDC (7-DHC-enriched medium) and of 124 μg/mL for NaUDC alone (7-DHC-free medium), respectively. To obtain a medium containing 19.2 μg/mL 7-DHC and 124 μg/mL NaUDC, the FBS containing 7-DHC at 385 μg/mL was diluted (1:1) with 7-DHC-free FBS. The solutions of 7-DHC-enriched medium and of 7-DHC-free medium were incubated at 4° C over-night before use.

2.3 Cell culture

The human melanoma cell line A2058, kindly provided from CEINGE (Naples, Italy) and SAN [32] were derived from lymphonodal metastasis. A2058 and SAN melanoma cells were grown in DMEM or RPMI, respectively, supplemented with 10% FBS, 2 mM L-glutamine, 100 IU/mL penicillin G and 100 μg/mL streptomycin in humidified incubator at 37 °C under 5% CO_2 atmosphere. They were split and seeded in plates (75 cm^2) every three days and used for assays during exponential phase of growth. Cell treatments were always carried after 24 hours from plating. A2058 or SAN cells were treated with culture media containing 19.2 μg/mL or 38.5 μg/mL of 7-DHC and 124 μg/mL of NaUDC, and with 7-DHC-free media as controls for 12, 24, 48, and 72 hours.

2.4 MTT assay

The 3-(4,5-dimethylthiazole-2-yl)-2,5-biphenyl-tetrazolium bromide (MTT) assay was used to detect cell proliferation. Cells were plated in 96-well at 2 x 10^4 cells/well and after one day-plating, 7-DHC was added to the cultures. At the end of each incubation time, MTT assay was performed according to the manufacturer's protocol. The absorbance

was measured at a wavelength of 570 nm with the ELISA plate reader (BioRad, Milano, Italy).

2.5 LDH Assay

A2058 cells were plated in 6-well at 1 x 10^5 cells/well and after one day-plating, 7-DHC was added to the cultures and cells were incubated for different times. At the end of each incubation, cytotoxicity was quantitatively assessed by measurements of lactate dehydrogenase (LDH) activity released in the extracellular fluid from damaged or destroyed cells [33]. Briefly, different aliquots of cell incubation media were added to a 1-mL reaction mixture containing 0.1M Tris-HCl, pH 7.5, 125 μM NADH, and incubated for 15 min at 30 °C. The reaction started with the addition of 600 μM sodium pyruvate and was followed by the decrease in absorbance at 340 nm. The results were normalized to 100% death caused by cell sonication.

2.6 Evaluation of Apoptosis

Annexin V-FITC was used to evaluate apoptosis during 7-DHC treatment. Briefly, cells were seeded into 6-well plate (2 x 10^5 cells/well) and treated with 7-DHC for 24 hours. After treatment, cells were washed twice with PBS, and harvested with a cell scraper. 1 x 10^5 cells were resuspended in 100 μL of 1 x binding buffer (10 mM Hepes pH 7.5, 140 mM NaCl, 2.5 mM $CaCl_2$) containing 5 μL of Annexin V-FITC and 10 μL of 50 μg/mL PI and incubated for 15 min at room temperature in the dark, and analyzed by flow cytometry. Apoptosis was further evaluated by determining the number of nuclei with a hypodiploid content of DNA using PI staining. Briefly, 7-DHC-treated cells were seeded into 96-well plates (2 x 10^4 cells/well); at the end of each treatment, cell suspensions were centrifuged and pellets were re-suspended in a hypotonic lysis solution containing 50 μg/mL propidium iodide. After incubation at 4 °C for 30 min, cells were analyzed by flow cytometry to evaluate the presence of nuclei with a DNA content lower than the diploid [34]. The effect of 7-DHC on apoptosis was also evaluated in the presence of NAC as antioxidant or apocynin as inhibitor of NADPH oxidase. In particular, the cells were pre-incubated for 1 hour with NAC (10 mM) or 45 min with apocynin (0.5 mM). After, the media were withdrawn and cells were treated with 7-DHC.

2.7 Measurements of caspase-3 activity

To evaluate caspase-3 activation during 7-DHC treatment, the enzymatic activity was measured by using caspase-3 fluorometric assay kit according to the manufacturer's protocol. Briefly, cells were seeded into 75 cm^2 plates (1 x 10^6 cells/plate) and treated with 38.5 µg/mL 7-DHC. At the end of incubation cells were collected, washed with PBS, and finally lysed at 4 °C using cell lysis buffer. Cell lysates (150 µg of proteins) were incubated with 50 µM DEVD-AFC substrate at 37 °C for 2 hours, to detect caspase-3 activity. The measurements were realized with a Cary Eclipse fluorescence spectrophotometer (Varian). Excitation and emission wavelengths were 400 nm and 505 nm, respectively; both excitation and emission slits were set at 10 nm.

2.8 Detection of intracellular ROS content

The intracellular ROS level was detected using the oxidation-sensitive fluorescence probe DCFH-DA. Briefly, A2058 cells were seeded into 6-well plate (1 x 10^5 cells/well) and treated with 7-DHC for different times. DCFH-DA was added in the dark at 10 µM final concentration 30 min before the end of each incubation; then cells were collected, washed in 10 mM sodium phosphate, pH 7.2 buffer containing 150 mM NaCl (PBS), and finally resuspended in 500 µL of PBS for the fluorimetric analysis. The measurement of the ROS levels was realized with a Cary Eclipse fluorescence spectrophotometer (Varian). Excitation and emission wavelengths were 485 nm and 530 nm, respectively; both excitation and emission slits were set at 10 nm. The effect of 7-DHC on ROS production was also evaluated pre-treating the cells with NAC (10 mM) or apocynin (0.5 mM) for 1 hour or 45 min, respectively. After, the media were withdrawn and cells were treated with 7-DHC.

2.9 Measurement of intracellular glutathione content

Intracellular glutathione content was measured using the EnzyChrome GSH/GSSG assay kit. Briefly, 2 x 10^6 cells were treated with 7-DHC (38.5 µg/mL) and after the incubation time they were sonicated and homogenized in phosphate buffer 50 mM and 1 mM EDTA. The suspension was centrifuged at 4° C for 15 min at 10,000 g, and the supernatant was deproteinized with 5% meta-phosphoric acid, centrifuged at 14,000 rpm for 5 min, and GSH and GSSG contents were measured following manufacturer's protocol.

2.10 Evaluation of mitochondrial membrane potential

Mitochondrial membrane potential was evaluated by measuring the incorporation of the fluorescent probe R123. Briefly, cells were seeded into 6-well plate (1 x 10^5 cells/well), incubated at 37 °C for 1 hour in the presence of 5 μM R123, washed twice with PBS and placed in medium containing 7-DHC. After different times of treatment, the medium was withdrawn and collected cells were washed twice with PBS. After detachment with trypsin, cells were harvested in PBS and centrifuged at 4 °C for 10 min. Following aspiration of supernatant, the cellular pellet was resuspended in 500 μL of PBS. The fluorescence of cell-associated R123 was measured in the above-mentioned fluorescence spectrophotometer, using excitation and emission wavelengths of 490 nm and 520 nm, respectively; both excitation and emission slits were set at 10 nm. The fluorescence intensities were normalized versus the cell number.

2.11 Total cell lysates and subcellular fractionation for Western blot analysis

A2058 cells were plated at a density of 1 x 10^5 cells/well in 6-well plates, treated and untreated cells were then harvested, washed with PBS, and lysed in ice-cold modified RIPA buffer (50mM Tris-HCl, pH 7.4, 150mM NaCl, 1% Nonidet P-40, 0.25% sodium deoxycolate, 1mM Na_3VO_4, and 1mM NaF), supplemented with protease inhibitors and incubated for 30 min on ice. The supernatant obtained after centrifugation at 12,000 g for 30 min at 4 °C constituted the total protein extract. Protein concentration was determined by the method of Bradford [35], using BSA as calibrator.

To obtain cytosolic and mithocondrial fractionation, cells were plated at a density of 2 x 10^6 cells/plate (143 cm^2). After the treatment, the cells were harvested, washed in PBS and then re-suspended in buffer M (5 mM Hepes, pH 7.4, 250 mM mannitol, 0.5 mM EGTA, 0.1% BSA), supplemented with protease inhibitors, and homogenized. The homogenate was centrifuged at 800 g for 10 min at 4 °C and the supernatant was then centrifuged at 12,000 g for 30 min at 4 °C. The resulting supernatant represented the cytosolic fraction, whereas the pellet constituting the mitochondrial fraction was resuspended in RIPA buffer.

To obtain nuclear and cytosolic extracts, cells plated at a density of 2 x 10^6 cells/plate (143 cm^2) were harvested and washed with PBS. Cells were resuspended with lysis buffer (10 mM Tris HCl, pH 7.5, 2 mM $MgCl_2$, 3 mM $CaCl_2$, 0.3 M sucrose), supplemented with 1 mM DTT and protease inhibitors, and homogenized. The homogenate was centrifuged

at 10,000 g for 20 min at 4 °C and the supernatant (cytosolic fraction) transferred in a clean tube. Then, the nuclei pellet was resuspended in extraction buffer (20 mM HEPES, pH 7.9, 1.5 mM $MgCl_2$, 0.42 M NaCl, 0.2 mM EDTA, 25% (v/v) glycerol), supplemented with 1 mM DTT and protease inhibitors, shaken gently for 30 min at 4 °C and centrifuged at 20,000 g for 5 min at 4 °C. The resulting supernatant represented the nuclear fraction. Equal amounts of total, cytosolic, mitochondrial, and nuclear protein extract were used for Western blot analysis. Briefly, protein samples were dissolved in SDS/reducing loading buffer, run on a 12% SDS-PAGE, then transferred to Immobilon P membrane (Millipore, Vimodrone MI, Italy). The filter was incubated with the specific primary antibody at 4 °C overnight and with the horseradish peroxidase-linked secondary antibody at room temperature for 1 hour. Membranes were then analyzed by an enhanced chemiluminescence reaction, using Super SignalWest Pico kit (Pierce - Thermo Scientific, Rockford, IL USA) according to the manufacturer's instructions; signals were visualized by autoradiography.

2.12 Immunofluorescence and confocal microscopy

Cells were plated on coverslips at a density of 0.3 x 10^6 cells/well in 6-well plates. At the end of the treatment for 24h, cells were incubated with 90 nM MitoTracker Red (Invitrogen) at 37 °C for 1 hour and then washed three times with ice-cold PBS. The cells were fixed with 4% paraformaldehyde, permeabilized with 0.1% Triton X-100 and blocked in donkey serum (Millipore) diluted 1:10 in PBS, for 60 min at room temperature. Coverslips were incubated for 1 hour at 37 °C with a primary rabbit polyclonal antibody against AIF, diluted 1:50 in PBS, and subsequently incubated for 1 hour at 37 °C with a FITC donkey anti-rabbit secondary antibody (Jackson ImmunoResearch Europe Ltd.), diluted 1:100 in PBS. At the end, nuclei were labelled with 4',6-diamidino-2-phenylindole (DAPI) for 15 min at room temperature. Slide mounting was done in Vectashield (Burlingame, CA, USA). Fluorescent-labeled cells were viewed with a confocal laser scanner microscope (Zeiss LSM 700, Jena, Germany) and the objective used was EC Plan-neofluar 40X/1.30 oil. The laser line was set at 488 nm for the FITC-conjugated antibody, at 555 nm for MitoTracker Red and 405 nm for DAPI. Images were acquired simultaneously in the green, red and blue channels, and as z-stack. Pictures were processed using ImageJ software (NIH, USA) to reconstruct x-axis projection using stack images.

2.13 Free sterol and sterol-derived compound analysis

Cells were plated at a density of 1 x 10^6 cells/plate (75 cm^2). Control cells, 7-DHC-treated cells (38.5 μg/mL), and respective culture media, were harvested protecting them from direct light. The cells were washed with PBS to eliminate traces of medium. To avoid sterol oxidation, BHT was suddenly added to cell and medium samples to provide a final concentration of 3 g/L. The cells were disrupted with mechanical techniques (freezing-defrosting, sonicating), and homogenized using a mini-potter on ice; the protein concentration in cell homogenates was determined by the method of Bradford [35].

7-DHC and cholesterol analysis was performed using 20 μL of vehicle suspension or 200 μL of medium or 100 μL of cell homogenate samples mixed with 25 μL of internal standard, 1 mL of ethanol containing 3 g/L BHT, and 1 mL of distilled water; the solution was extracted with hexane (3 x 2 mL). The upper organic phases were pooled and evaporated under a gentle stream of nitrogen. The dry residue was reconstituted with 50 μL of dichloromethane, and 1 μL of the resulting solution was injected into the GC-FID.

The extraction of oxidized sterol compounds, after hydrolysis, was performed according to Pulfer and Murphy procedure [36]. One-hundred μL of medium or cell homogenate samples were mixed with 25 μL of IS and hydrolyzed for 60 min at 80 °C in 2 mL of 1N KOH in 90% methanol containing 3 g/L BHT. After the hydrolysis, the sample was diluted with 2 mL of distilled water, and extracted with dichloromethane (3 mL followed by 2 mL two times). The lower phases were pooled and evaporated under a gentle stream of nitrogen. The dry residue was derivatized by the addition of 30 μL pyridine and 70 μL BSTFA followed by a heating at 80 °C for 30 min. The derivatized sample was dried under nitrogen stream and the residue was dissolved with 50 μL dichloromethane; 1 μL of the solution was injected into the GC-FID and GC-MS.

2.14 Gas chromatography (GC-FID and GC-MS)

Free sterol analysis was performed as previously described [9]. Briefly, a gas chromatograph equipped with a flame ionization detector (GC-FID, HP-5890, Agilent Laboratories, CA, USA) equipped with a SAC-5 capillary column (30 m length, 0.25 mm I.D., 0.25 μm film thickness; Supelco, Germany), was used to separate the sterols using nitrogen as carrier gas. The linear velocity of carrier gas was 45 cm/s.

Injector and detector temperatures were fixed at 300 °C, and the oven temperature at 290 °C for a total run time of 30 min. Sterol concentrations were obtained by interpolating the peak area ratios (analyte/IS) on the calibration curves. The sterol-derived compounds were analyzed by GC-FID (HP-5890) and by GC-MS controlled by a work station using MassLab 3.4 as software (Fisons, model GC 8000/MD800). Chromatography conditions of GC-MS apparatus were as above described and using helium carrier gas. Qualitative analysis was performed by GC-MS scanning the mass range from m/z 50 to 600 comparing compound mass spectra with those reported into mass spectra libraries (Wiley and National Institute of Standards and Technology). Quantitative analysis was performed using GC-FID, compound identification was obtained by the relative retention time (Rf=Rt analite/Rt IS). Oxidized sterol compound concentrations were calculated from the ratio of peak area compared to calibration curves of oxysterols (cholesterol 5β,6β-epoxide, 25-hydroxy-cholesterol, and 7-keto-cholesterol).

2.15 Liquid chromatography tandem mass spectrometry (LC-MS/MS)

The oxidized sterol compounds were also analyzed by LC-MS/MS using a slight modification of the method of Pulfer and Murphy [36]. Briefly, the dried extracts were dissolved in 200 µl ethanol, then 5 µl were injected onto a reverse phase column (Zorbax Eclipse® Plus C18, 3.5 µm, 150 x 2.1 mm; Agilent Technologies, Cernusco, Italia) at a flow rate of 0.3 mL/min. Solvent A was methanol/water/acetonitrile (v/v/v, 60:20:20) with 4 mM ammonium acetate; solvent B was methanol with 4 mM ammonium acetate. The gradient ran from 90 to 100% solvent B in 10 min and stayed at 100% solvent B for 10 min. Multiple reaction monitoring analysis was carried out on a Quattro-Micro mass spectrometer (Waters Corporation, Milford, USA). The mass spectrometer operated in positive ion mode by atmospheric pressure chemical ionization probe (APCI). The cone voltage was set at 25 V, the collision energy at 20 eV and the gas cell Pirani gauge at 2.2 x 10-3 mbar using argon as the collision gas. Source temperature, desolvation gas flow rate, desolvation gas temperature, cone gas flow rate and gas nebulizer pressure were set at 120 °C, 350 L/h, 350 °C, 50 L/h and 80 psi, respectively, while the corona discharge was set at 2 mA. Multiple reaction monitoring (MRM) transitions were m/z 385 > 367 for 7-DHC, 25-hydroxy-cholesterol, and 5β,6β-epoxide, m/z 399 > 381 for 3β,5α-

dihydroxycholest-7-en-6-one (DHCEO) and 7-keto-dehydro-cholesterol (7-keto-DHC), and m/z 401 > 383 for 25-hydroxy-7-DHC and 7-keto-cholesterol. The dwell time for each transition was 100 ms. Quantitative analysis was carried out using calibration curves of 25-hydroxy-cholesterol for 25-hydroxy-7-DHC, and of 7-keto-cholesterol for DHCEO and 7-keto-DHC.

2.16 Statistical analysis

Data are reported as average, standard deviation, and standard error. The statistical significance of differences among groups was evaluated using the ANOVA, with the Bonferroni correction as post-hoc test, or the Student's t-test where appropriate. The significance was accepted at the level of $p < 0.05$.

3. Results

3.1 Study on 7-DHC stability

In order to evaluate the 7-DHC stability, we monitored the 7-DHC concentration in the suspension of NaUDC/7-DHC used to prepare 7-DHC-enriched media. The suspension was stored at 4°C up to three months. The average concentration of 7-DHC suddenly after the preparation of the suspension was 3.97 ± 0.01 g/L. As shown in figure 1, no significant changes from baseline values were observed in the 7-DHC levels in the suspension up to 90 days of storage at 4 °C.

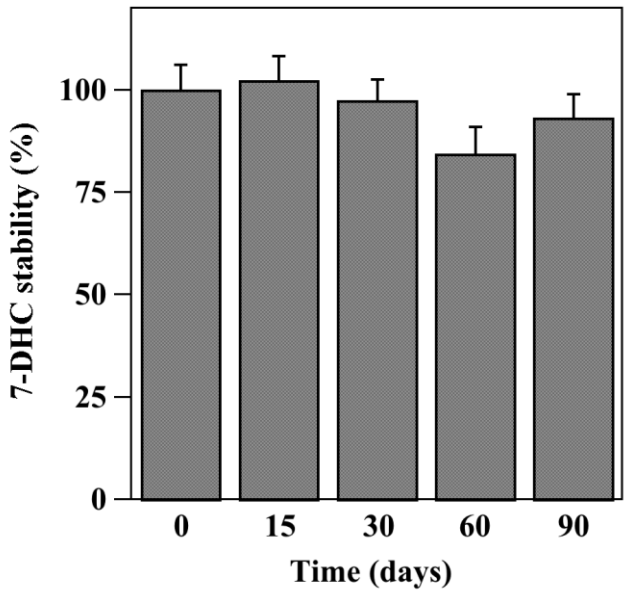

Fig. 1 Time-course of 7-DHC level in the NaUDC/7-DHC suspension
7-DHC concentrations were determined by GC-FID method and were expressed as percentage of average baseline values (3.97 g/L). Data from quadruplicate experiments are reported as mean ± SE.

3.2 Sterol levels in culture media and melanoma cells

It is known that handling of 7-DHC in culture media may lead to its disruption/conversion into derivative compounds [12]. Therefore, in order to assess the correlation between the levels of 7-DHC and its effects on melanoma cells, we monitored by GC-FID the levels of cholesterol and 7-DHC in culture media and cells of experiments carried out in this work. The quantitative analysis of free sterols was made at baseline and during the time-course of stimulation. The levels of cholesterol in the culture media from 7-DHC-treated melanoma cells were almost unchanged during the first 12 hours, then the levels decreased progressively up to 67% after 72 hours (Table 1).

Table 1. Cholesterol levels in 7-DHC-treated and untreated cells and media

	basal	12h	24h	48h	72h
CHOL in cells			μg/mg of proteins (SE)		
Treated	24.2 (2.4)	35.0 (1.8)	34.2 (1.9)	29.7 (2.7)	37.4 (4.7)
Untreated	24.2 (2.4)	28.0 (1.2)	24.2 (1.7)	25.7 (0.1)	26.4 (5.2)
*p		0.03	0.01	0.34	0.22
CHOL in media			μg/mL (SE)		
Treated	8.2 (0.4)	8.0 (0.1)	7.2 (0.5)	5.9 (0.6)	5.5 (0.8)
Untreated	8.0 (0.1)	8.2 (0.2)	8.5 (0.3)	5.2 (0.7)	5.4 (1.4)
*p	0.76	0.44	0.12	0.49	0.96

The micromoles of cholesterol can be obtained dividing the values by the molecular weight of 386.6 Da. * Statistical significance.

A similar behavior was essentially observed in media from untreated cells. On the other hand, cholesterol levels in untreated or treated melanoma cells were stable during the whole incubation time, independently of some differences observed in the basal levels of this sterol measured between untreated and treated cells. However, these variations were significant only at the incubation times of 12 and 24 hours (Table 1). Concerning the levels of 7-DHC, the corresponding values measured in media and cells are shown in Table 2.

Table 2. Total amounts and percentages of 7-DHC in treated cells and media

	basal	12h	24h	48h	72h
7-DHC			μg (SE)[a]		
Media	272.4 (20.2)	37.8 (0.9)	36.0 (4.2)	17.2 (7.4)	18.9 (9.0)
Cells	-	223.3 (2.0)	224.8 (6.2)	230.3 (15.1)	234.7 (14.5)
			Average %		
Media	100	13.9	13.2	6.3	6.9
Cells	-	82.0	82.5	84.6	86.2
Δ	-	4.1	5.4	6.4	6.9

a: Total micrograms (standard error) of 7-DHC in media and cells as averages/well.
Δ: 7-DHC gap as: (7-DHC basal in media) - (7-DHC in media + 7-DHC in cells).
The micromoles of 7-DHC can be calculated dividing the values by 384.6 Da (molecular weight).

The comparison of these data suggests that 7-DHC moved from media to cells and that, after 12 hours of treatment, a great percentage of this sterol (82%) already entered the cell; the influx reached 86% after 72 hours.
However, as reported in Table 2, a gap of 7-DHC was observed between total amount at basal state in the culture media and the sum of 7-DHC found in media and treated cells at different incubation times. This gap ranged between 4.1% and 6.9% during the whole incubation time. These results could indicate the presence of other sterol compounds, which were determined both by GC-MS and LC-MS/MS. At basal state the medium enriched with 7-DHC contained 5.67 μg/well of cholesta-4,6,8(14)-trien-3ol, 5.44 μg/well of cholesta-5,7,9(11)-trien-3ol, and 1.80 μg/well of cholesta-5,8,24-trien-3ol. During the time-course of treatment these compounds entered rapidly the cells reaching on average a percentage of 44%, 72%, and 83%, respectively. In addition, a new metabolite was found into the cells. This compound, identified as 25-hydroxy-7-DHC, was undetectable in media and its quantity ranged between 2.90 and 5.26 μg/well (Table 3). As reported in Table 4, the analysis performed by LC-MS/MS confirmed this result, and showed that the medium enriched with 7-DHC, at basal state, contained on average 3.06 μg/well of 7-keto-cholesterol, 0.68 μg/well of DHCEO, and 0.11 μg/well of 7-keto-DHC. After 72 hours of treatment with 7-DHC, the cells contained these compounds in part as influx from the medium and in part as metabolites produced from cholesterol and 7-DHC. Since the amount of each compound in the medium was on average always less than 1 μg/mL (8 mL/well), this concentration was not considered toxic for cell growth.

Table 3. Levels of sterol-derived compounds in 7-DHC-treated cells and media analyzed by GC-FID and GC-MS

	Cholesta-4,6,8(14)-trien-3-ol		Cholesta-5,7,9(11)-trien-3-ol		Cholesta-5,7,24-trien-3-ol		25-hydroxy-7-DHC	
	μg (SE)[a]							
Incubation times	**Media**	**Cells**	**Media**	**Cells**	**Media**	**Cells**	**Media**	**Cells**
basal	5.67 (0.51)	-	5.44 (0.24)	-	1.80 (0.08)	-	-	-
12 hours	1.76 (0.37)	2.31 (0.25)	1.75 (0.51)	3.15 (0.13)	-	1.16 (0.04)	-	5.26 (0.11)
24 hours	2.10 (0.27)	2.48 (0.27)	1.86 (0.20)	3.57 (0.01)	-	1.34 (0.09)	-	2.90 (0.03)
48 hours	1.10 (0.08)	2.39 (0.25)	2.34 (0.16)	3.08 (0.19)	-	1.45 (0.03)	-	4.40 (1.00)
72 hours	0.77 (0.02)	2.49 (0.21)	1.58 (0.02)	3.91 (0.14)	-	1.49 (0.26)	-	4.86 (1.13)

a: Total micrograms (standard error) of each sterol-derived compound in media and cells as average/well (n=3). The micromoles of compounds can be obtained dividing the values by the following molecular weights (Da): 382.6 for Cholesta-4,6,8(14)-trien-3-ol, Cholesta-5,7,9(11)-trien-3-ol, and Cholesta-5,7,24-trien-3-ol; and 400.6 for 25-hydroxy-7-DHC.

Table 4. Levels of sterol-derived compounds in 7-DHC-treated cells and media analyzed by LC-MS/MS

	25-hydroxy-7-DHC		7-keto-cholesterol		DHCEO		7-keto-DHC	
Incubation times	μg (SE)[a]							
7-DHC-Treated	**Media**	**Cells**	**Media**	**Cells**	**Media**	**Cells**	**Media**	**Cells**
basal	-	-	3.06 (0.28)	0.13 (0.01)	0.68 (0.03)	-	0.11 (0.01)	-
72 hours	-	4.42 (0.99)	0.90 (0.08)	0.48 (0.04)	0.56 (0.04)	0.76 (0.02)	0.16 (0.01)	0.04 (0.01)
Untreated								
basal	-	-	4.89 (0.44)	0.13 (0.01)	-	-	-	-
72 hours	-	-	4.65 (0.39)	0.16 (0.01)	-	-	-	-

a = Total micrograms (standard error) of each sterol-derived compound in cells and media as average/well (n=3). The micromoles of compounds can be obtained dividing the values by the following molecular weights (Da): 400.6 for 25-hydroxy-7-DHC and 7-keto-cholesterol, 416.6 for DHCEO, and 398.6 for 7-keto-DHC.

3.3 Cytotoxic effect of 7-DHC in melanoma cell lines

To investigate if the treatment of A2058 melanoma cells with 7-DHC affects cell viability, a MTT assay was performed. To this aim, melanoma cells were incubated for 24 and 48 hours with two different concentrations of 7-DHC (19.2 or 38.5 μg/mL) or with the vehicle alone. The spectrophotometric analysis showed a decrease of cell proliferation after 24 hours only in the presence of 38.5 μg/mL 7-DHC, whereas after 48 hours of incubation with 7-DHC, a dose-dependent decrease of cell growth was observed (Fig. 2).

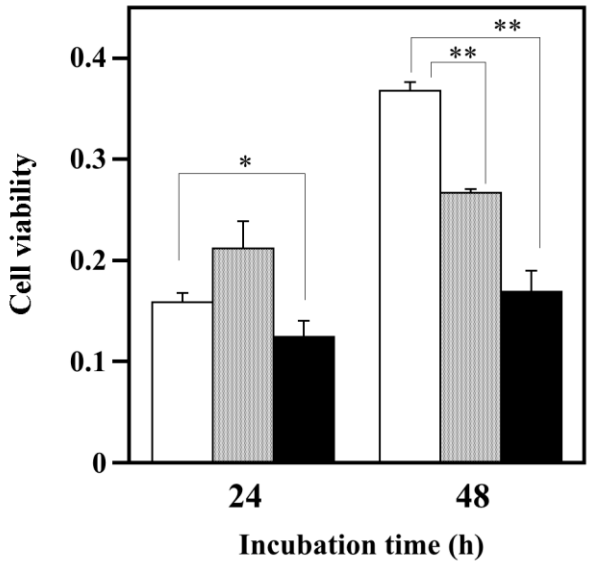

Fig. 2 Effect of 7-DHC on cell viability of A2058 melanoma cells
A2058 cells were incubated for 24 and 48 hours with vehicle alone (white bars), 19.2 μg/mL (grey bars) or 38.5 μg/mL (black bars) 7-DHC. Cell viability was evaluated by MTT assay and was reported as arbitrary units (a.u.). Data from triplicate experiments are reported as mean ± SD. *$p < 0.05$ and **$p < 0.01$ compared to untreated cells.

These results suggest that the treatment of A2058 cells with 7-DHC could exert a cytotoxic effect on this melanoma cell line. In addition, the cytotoxic effect of 7-DHC has been also confirmed on SAN melanoma cells and the results were comparable to that obtained on A2058 cell line (Fig. 3).

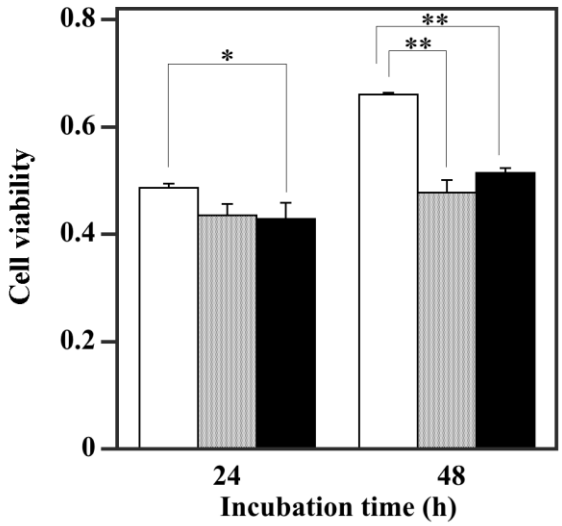

Fig. 3 Effect of 7-DHC on cell viability of SAN melanoma cells
SAN cells were incubated for 24 and 48 hours with vehicle alone (white bars), 19.2 µg/mL (grey bars) or 38.5 µg/mL (black bars) 7-DHC. Cell viability was evaluated by MTT assay and was reported as arbitrary units (a.u.). Data from triplicate experiments are reported as mean ± SD. *$p < 0.05$ and *$p < 0.01$ compared to untreated cells.

We have evaluated if the reduction of cell proliferation induced by the 7-DHC treatment of A2058 cells could be indicative of a cell death process. It is known that LDH activity significantly increases in culture media of cells undergoing a necrosis. Therefore, we have assayed the LDH activity in culture media from A2058 cells incubated up to 48 hours with 38.5 µg/mL of 7-DHC. However, the results showed a not significant release of LDH from A2058 cells treated with 7-DHC compared to untreated cells (Table 5).

Table 5. LDH activity in untreated and 7-DHC-treated A2058 culture media

	Untreated	**7-DHC-treated**	
		19.2 mg/mL	38.5 mg/mL
Incubation times		IU/L (SE)	
24 hours	78 (1.5)	76 (2.0)	75 (2.8)
48 hours	93 (0.3)	95 (2.0)	98 (1.2)

Differences among groups were not statistically significant (ANOVA).

Then, we analyzed the exposure of phosphatidylserine moieties on cell membranes, identified by Annexin V binding, after cell treatment with 7-DHC. As shown in Fig. 4a the treatment of A2058 cells with 19.2 or 38.5 µg/mL 7-DHC for 24 hours induced a significant increase of the percentage of early apoptotic cells (Annexin+/PI−), whereas the increase of percentage of late apoptotic cells (Annexin+/PI+) was low even if significant after treatment with 19.2 µg/mL 7-DHC.

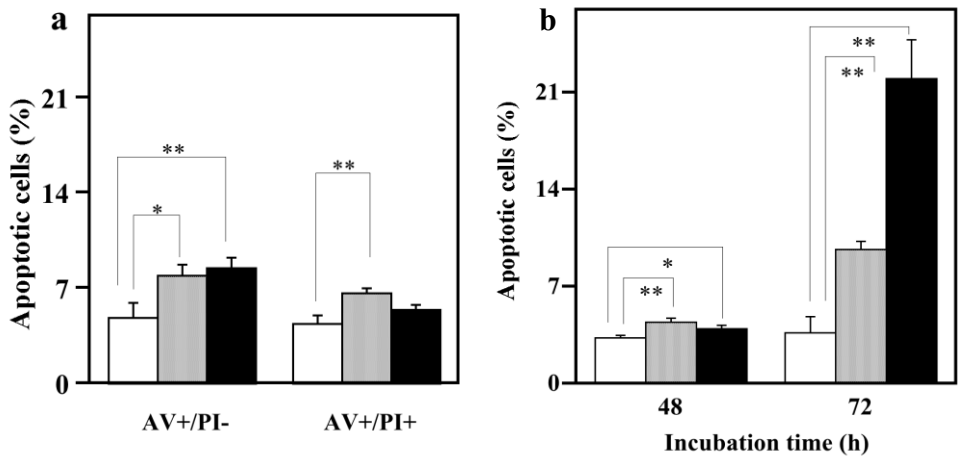

Fig. 4 Pro-apoptotic effect of 7-DHC on A2058 melanoma cells
a) A2058 cells were incubated for 24 hours with vehicle alone (white bars), 19.2 µg/mL (grey bars) or 38.5 µg/mL (black bars). Annexin V-FITC binding and the propidium iodide incorporation were evaluated cytofluorimetrically. Annexin V-positive/PI negative cells (AV+/PI-) and Annexin V-positive/PI positive cells (AV+/PI+) represent early and late apoptotic cells, respectively. The data were expressed as percentage. **b)** A2058 cells were incubated for 48 and 72 hours with vehicle alone (white bars), 19.2 µg/mL (grey bars) or 38.5 µg/mL (black bars) 7-DHC. PI staining and cytofluorimetric analysis were used to evaluate the number of nuclei with a hypodiploid content of DNA and the data were expressed as percentage. Data from triplicate experiments are reported as mean ± SD. *$p < 0.05$ and **$p < 0.01$ compared to untreated cells.

Furthermore, flow cytometric analysis of PI incorporation on A2058 cells, incubated with 19.2 or 38.5 µg/mL 7-DHC for different times, showed that the number of nuclei with sub-diploid DNA content started to increase after 48 hours of treatment compared to untreated cells, and after 72 hours a dose-dependent effect was evident (Fig. 4b). The same effect was observed on SAN melanoma cells after 48 hours of treatment with 38.5 µg/mL of 7-DHC (Fig. 5).

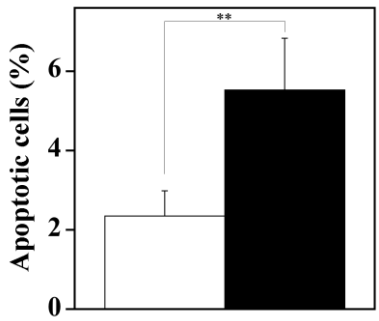

Fig. 5 Pro-apoptotic effect of 7-DHC on SAN melanoma cells
SAN cells were incubated for 48 hours with vehicle alone (white bars) or 38.5 μg/mL (black bars) 7-DHC. PI staining and cytofluorimetric analysis were used to evaluate the number of nuclei with a hypodiploid content of DNA and the data were expressed as percentage. Data from triplicate experiments are reported as mean ± SD. **$p < 0.01$ compared to untreated cells.

These data are indicative that the effect of 7-DHC may be mainly due to an apoptotic process.
As activation of caspase is one of the widely recognized features of apoptosis [37], the enzymatic activity of caspase-3 was measured after 7-DHC treatment. However, A2058 cells, incubated with 19.2 or 38.5 μg/mL 7-DHC for different times, didn't show any significant variation of caspase-3 activity.
Furthermore, since caspase-3 mediates the cleavage of PARP-1, we evaluated the inactivation of PARP-1 analyzing in nuclear and cytosolic fractions both 116 kDa and 89 kDa forms, which represent the uncleaved and cleaved form of PARP-1, respectively. Western blot analysis showed the presence of PARP-1 as intact protein in nuclear fraction (116 kDa), while PARP-1 cleaved fragment (89 kDa) was not detected in both nuclear and cytosolic extracts (Fig. 6). Hence, these data are indicative that the 7-DHC affects the viability of the A2058 likely in a caspase-independent manner.

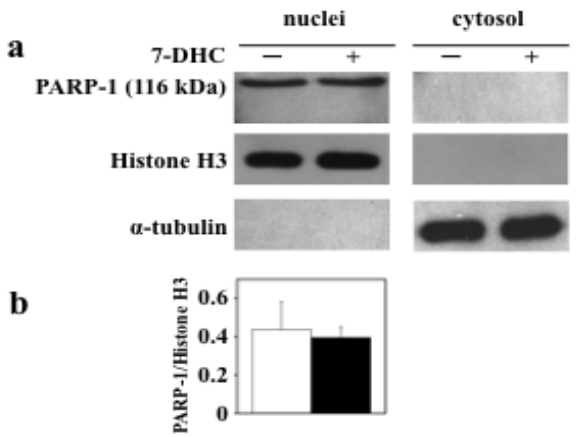

Fig. 6 Effect of 7-DHC on PARP-1 protein levels in nuclear and cytosolic fractions
A2058 cells were incubated for 24 hours with vehicle alone or 38.5 μg/mL 7-DHC. **a)** Nuclear and cytosolic protein extracts were used to perform PARP-1 Western blot analysis. Histone H3 and α-tubulin were utilized to evaluate the loading and purity of nuclear and cytosolic protein fractions, respectively. **b)** Densitometric analysis of PARP-1 protein levels in nuclear fraction. Data from triplicate experiments are reported as mean ± SD.

3.4 Effect of 7-DHC on the intracellular ROS and glutathione levels

Structure of 7-DHC is very similar to that of cholesterol, but 7-DHC is a molecule more reactive because of the presence in its structure of a conjugated double bound. Hence, high 7-DHC intracellular levels can affect the cellular physiology and in particular the intracellular redox state. In fact, 7-DHC may contribute to this process by replacing cholesterol in cell compartments and then altering signal transduction processes in lipid rafts generating oxidized 7-DHC derivatives [38].
To this aim, the intracellular ROS level was measured in A2058 cells treated with 7-DHC. In particular, the cells were incubated with 38.5 μg/mL of 7-DHC, and ROS production was detected at different times through the use of the fluorescent probe DCFH-DA (Fig. 7a). An increment of fluorescence intensity was clearly evident already after 2 hours of incubation; this increase remained up to 8 hours of 7-DHC treatment. Furthermore, ROS production induced by 7-DHC was also evaluated on cells pre-treated with NAC (10 mM) as antioxidant or apocynin (0.5 mM) as NADPH oxidase inhibitor. After 2 hours of treatment with 7-DHC, the pre-treatment with NAC or apocynin antagonized the 7-DHC effect and the ROS levels were unchanged respect to basal state (Fig. 7b).

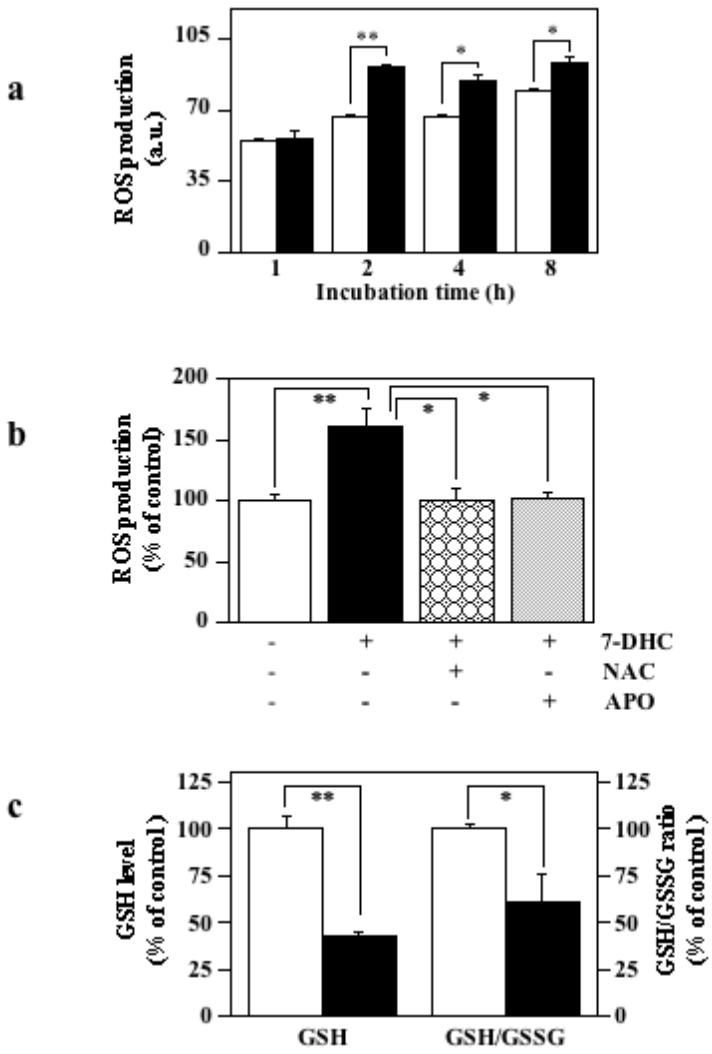

Fig. 7 Effect of 7-DHC on the intracellular ROS and glutathione levels
A2058 cells were incubated for the indicated time periods with vehicle alone (white bars) or 38.5 μg/mL 7-DHC (black bars). The fluorescent probe DCFH-DA was used to detect the intracellular ROS levels. Fluorescence intensity was reported as arbitrary units (a.u.) (**panel a**). A2058 cells were pre-incubated with the free radical scavenger, NAC (10 mM), or apocynin (0.5 mM), a NADPH oxidase inhibitor. The intracellular ROS level was evaluated after 2 hours of 7-DHC treatment by using the fluorescent probe DCFH-DA. ROS production was expressed as percentage of control (**panel b**). The intracellular GSH level and the GSH/GSSG ratio were evaluated after 2 hours of 7-DHC treatment. The data were expressed as percentage of control (**panel c**). Data from triplicate experiments are reported as mean ± SD. *$p < 0.05$ and **$p < 0.01$ compared to untreated cells.

These results suggest that 7-DHC alters the intracellular redox state and, in particular, the increase of ROS levels is mediated by NADPH oxidase.
In addition, to further evaluate the alteration of redox state by 7-DHC we measured the intracellular levels of GSH and GSH/GSSG ratio.
The results reported in Fig. 7c show that both GSH level and GSH/GSSG ratio were statistically reduced after 2 hours of 7-DHC treatment.

3.5 Effect of NAC and apocynin on apoptosis induced by 7-DHC

The alteration of redox state of melanoma cells induced by 7-DHC may represent an early event that can contribute to affect the cell viability. Therefore, we investigated if the apoptotic effect of 7-DHC is antagonized by NAC (10 mM) or apocynin (0.5 mM) pre-treatment. As reported in Fig. 8, the pro-apoptotic effect on A2058 cells treated for 72 hours with 38.5 μg/mL 7-DHC was partially but significantly reduced by both NAC and apocynin pre-treatment, even though the percentage of apoptosis observed in NAC and apocynin pre-treated cells was still and significantly higher compared to untreated control cells.

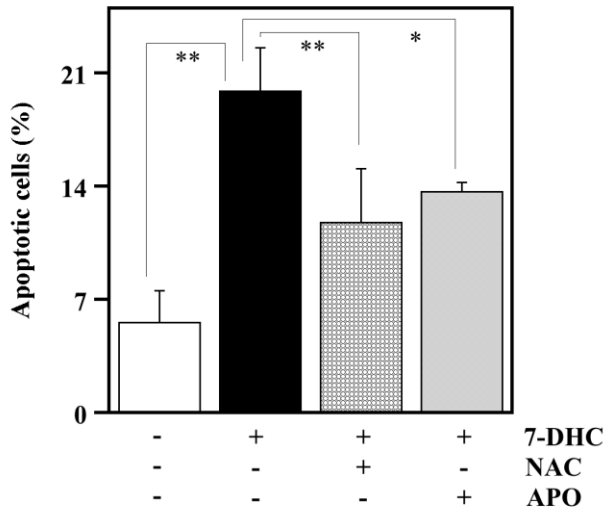

Fig. 8 Effect of NAC and apocynin on 7-DHC induced apoptosis
The apoptotic effect of 7-DHC was evaluated on A2058 cells pre-incubated with NAC (10 mM) or apocynin (0.5 mM) before the treatment with vehicle alone or with 38.5 μg/mL 7-DHC for 72 hours. Apoptosis was revealed by cytofluorimetric analysis and was expressed as percentage. Data from triplicate experiments are reported as mean ± SD. *$p < 0.05$ and **$p < 0.01$ compared to untreated cells.

3.6 Effect of 7-DHC on mitochondrial membrane potential

The mitochondria respiratory chain is the major source of cellular ROS; at the same time, mitochondria are also the main targets of ROS detrimental effects. Indeed, the increase of intracellular ROS levels represents one among the critical events that alter the mitochondrial membrane potential, thus contributing to trigger mitochondria dysfunction. Therefore, the effect of 7-DHC treatment on mitochondrial membrane potential of A2058 cells was evaluated by measuring the incorporation of the fluorescent probe R123. This compound crosses the mitochondrial membrane and accumulates into the matrix only when the trans-membrane potential is preserved; therefore, in case of a loss of the membrane potential, the R123 fluorescence undergoes a significant reduction [39]. Data reported in Fig. 9 indicated that the reduction of R123 mitochondrial incorporation in 7-DHC-treated cells was statistically significant compared to untreated cells. In fact, a decrease of mitochondrial membrane potential was detected in A2058 cells incubated for 24 and 48 hours with 38.5 μg/mL 7-DHC.

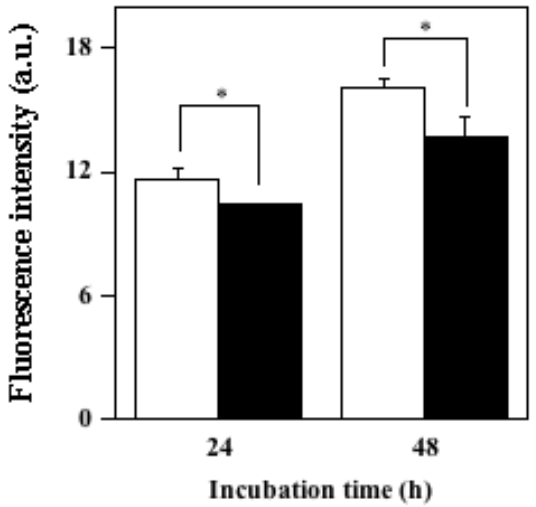

Fig. 9 Mitochondrial membrane depolarization induced by 7-DHC
A2058 cells were incubated for 24 and 48 hours with vehicle alone (white bars) or 38.5 μg/mL 7-DHC (black bars). The fluorescent probe R123 was used to evaluate the mitochondrial membrane potential. Fluorescence intensity was reported as arbitrary units (a.u.). Data from triplicate experiments are reported as mean ± SD. *$p < 0.05$ compared to untreated cells.

3.7 Effect of 7-DHC on levels and subcellular localization of some proteins involved in the apoptotic process

To obtain further insights on the molecular mechanisms activated by 7-DHC during cellular treatment, we have analyzed the levels of some proteins that regulate the apoptotic process. Proteins of Bcl-2 family play a key role in the intrinsic apoptotic process [40,41]; therefore, we have evaluated the protein levels of Bcl-2 and Bax, as well as the ratio Bcl-2/Bax, because Bcl-2 and Bax are considered typical anti-apoptotic and pro-apoptotic factors, respectively. As shown in Fig. 10a,b,c, the levels of Bcl-2 in total protein extract were unchanged in A2058 cells treated for 24 hours with 38.5 μg/mL 7-DHC, whereas the increased levels of Bax and the reduction of Bcl-2/Bax ratio were statistically significant in treated cells compared to untreated cells. In particular, as shown in Fig. 10d, in subcellular fractions of A2058 treated cells with 38.5 μg/mL 7-DHC for 24 hours, both cytosolic and mitochondrial levels of Bax were increased compared to untreated cells.

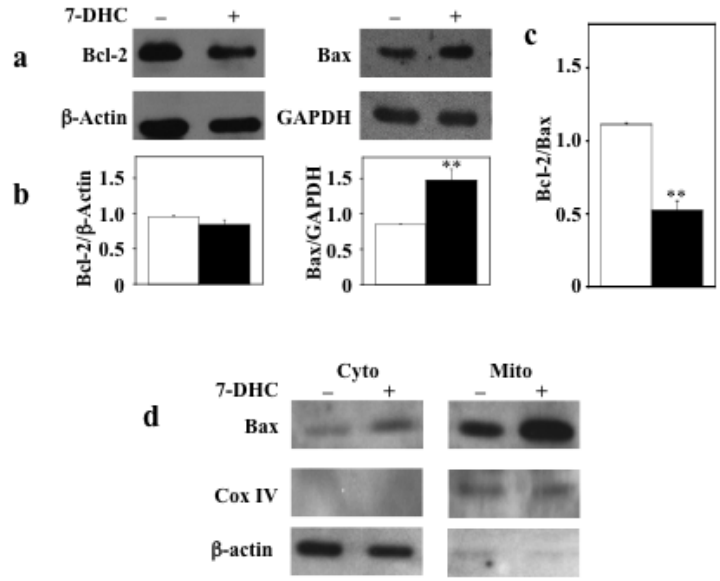

Fig. 10 Effect of 7-DHC on Bcl-2 and Bax intracellular protein levels
A2058 cells were incubated for 24 hours with vehicle alone or 38.5 μg/mL 7-DHC. **a)** Total proteins extracts were used to perform Western blot experiments. β-actin and GAPDH were utilized as loading control for Bcl-2 and Bax protein levels evaluation, respectively. **b)** Densitometric analysis of Bcl-2 and Bax protein levels. **c)** Determination of Bcl-2/Bax ratio.**d)** Bax protein levels in cytosolic and mitochondrial fractions. Mitochondrial marker COX-IV and the cytosolic marker β-actin were used to verify the purity of fractions as well as loading controls. Data from triplicate experiments are reported as mean ± SD. **$p < 0.01$ compared to untreated cells.

As 7-DHC treatment on A2058 cells did not have any effect on caspase-3 activation, we have analyzed the protein levels of AIF, a main mediator of caspase-independent cell death [42]. A2058 cells incubated with 38.5 µg/mL 7-DHC for 24 hours showed a statistically significant increase of AIF protein levels (Fig. 11). Furthermore, to verify the subcellular localization of AIF we performed immunofluorescence experiments by confocal microscopy. As showed in fig 12, AIF immunostaining is more evident in treated A2058 cells (panels d,e,f) compared to control cells (panels a,b,c). Furthermore, as better showed in 3D image of treated cells (panel e) and untreated cells (panel b), immunofluorescence analysis detected a nuclear AIF immunoreactivity only in the treated cells. These results support the hypothesis that cell death induced by 7-DHC may be mainly due to an apoptotic process caspase-independent.

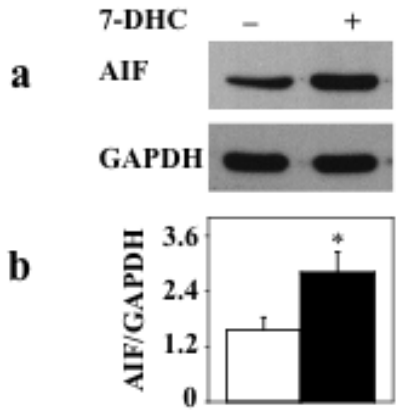

Fig. 11 Effect of 7-DHC on AIF intracellular protein levels
A2058 cells were incubated for 24 hours with vehicle alone or 38.5 µg/mL 7-DHC. **a)** Western blot analysis of AIF levels was performed on total protein extracts; GAPDH was used as loading control for protein levels evaluation. **b)** Densitometric analysis of AIF protein levels. Data from three independent experiments are reported as mean ± SD. *$p < 0.05$ compared to untreated cells.

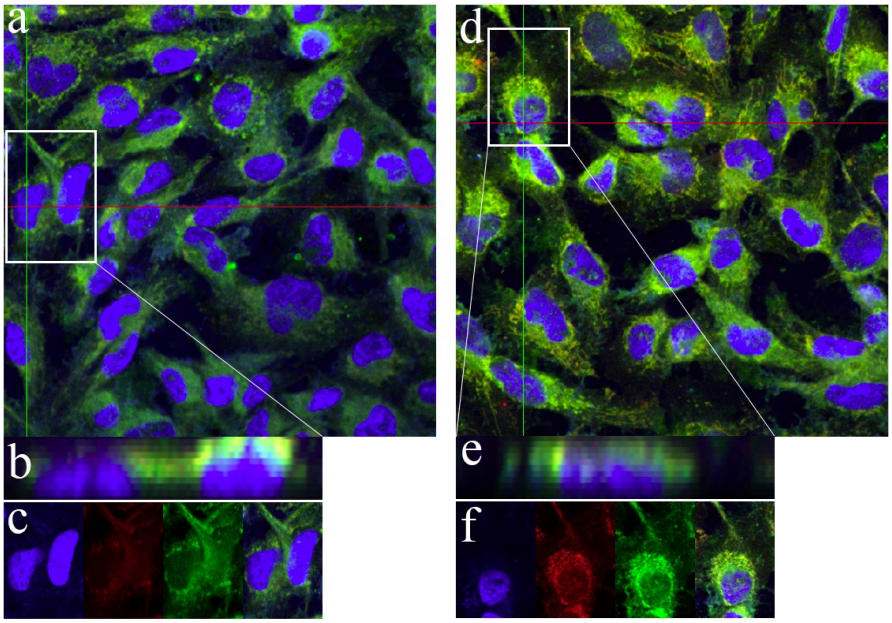

Fig. 12 Effect of 7-DHC on AIF subcellular localization
A2058 cells were treated for 24 hours with vehicle alone (**a, b, c**) or 38.5 μg/mL 7-DHC (**d, e, f**). Nuclei staining (blue fluorescence) was performed with 4', 6-diamidino-2-phenylindole (DAPI); mitochondria were stained with MitoTracker Red (red fluorescence); AIF immunostaining (green fluorescence) was performed using a monoclonal anti-AIF antibody, followed by FITC-conjugated antibody. The signals are showed as a merge (**a** and **d**), the cells in the inset are represented as x-axis volume projection (**b** and **e**), and as splitted channels (**c** and **f**). The shown results are representative of three independent immunofluorescence experiments.

4. Discussion and Conclusions

The skin plays a pivotal role to maintain the body homeostasis and contributes also to immune and neuroendocrine activities [20]. The exposure of skin to solar radiations (e.g. UV-A and -B) causes skin damage including oxidative stress, DNA damage, inflammation, melanoma, and non-melanoma skin cancer. The results presented here show that the 7-DHC, a lipophilic compound, affects the growth of A2058 melanoma cells in vitro at concentrations ranging from 19.2 to 38.5 μg/mL. The 7-DHC, or pro-vitamin D, is naturally present at physiological levels in the skin and, under UV exposure, it serves as the precursor for active metabolites that influence the formation and maintenance of barrier function and other activities such as anti-microbial, anti-senescence, and photoprotective of skin. In this work A2058 melanoma cells were treated with 7-DHC, in dark conditions, to assess its direct effect on vitality of this cancerous cell line.

In fact, the most of published work have tested the derivative products of 7-DHC induced by UV in cell models to assess the effects in keratinocyte, in which 7-DHC enhances UV-induced oxidative stress leading to inflammation producing more ROS, and cell death by a ROS and caspase-3 dependent apoptotic mechanism [10,26]. On the other hand, in keratinocytes, UV-B irradiation induces non-enzymatic isomerization of 7-DHC converting biologically inactive vitamin D3 to the hormone calcitriol (1α,25-dihydroxyvitamin D3) and to other vitamin D analogs. These compounds have antiproliferative and pro-differentiative effects on epidermal keratinocytes and have become potent therapeutic agents for the treatment of proliferative skin disorders [43] and malignant melanoma [44]. Instead, studies in which the 7-DHC has been directly used to evaluate its effects in cancer cells are lacking.

In this work we addressed the cellular mechanisms for responses, in vitro, of melanoma cells to 7-DHC to elucidate its cytotoxic and pro-apoptotic effects. We chose A2058 cells, a highly metastatic human amelanotic cell line, to examine the cytotoxicity of this lipophilic metabolite of cholesterol and vitamin D biosynthesis. 7-DHC levels used to stimulate melanoma cells mimicked those found in the blood of SLOS patients with low/mild increase of 7-DHC levels and 7-DHC/cholesterol ratio. It is known that 7-DHC is prone to oxidation and has a high oxidizing power [18,19]; therefore, in order to understand its direct effects and to reduce the formation of oxidized compounds we prepared a suspension using the NaUDC as vehicle to transfer the 7-DHC from the culture medium into

the cells. In fact, the suspension of NaUDC/7-DHC showed a higher stability of the compound during the storage at 4 °C up to three months (Fig. 1), even if its preparation was more laborious than other procedures.
We evaluated the cytotoxic potential of 7-DHC on A2058 melanoma cell line, as well as on SAN cell line, by monitoring the cell proliferating rate through the MTT assay. The data from these experiments indicated a decrease of cell proliferation after 24 hours in the presence of 38.5 μg/mL 7-DHC and after 48 hours of incubation with 7-DHC a dose-dependent decrease of cell viability was observed (Fig. 2,3). These results suggest that the treatment of cells with 7-DHC reduces the viability of these melanoma cell lines.
During the monitoring of lipids extracted from treated melanoma cells and culture media, we found that more than 82% of 7-DHC entered the cells already after 12 hours; this high percentage of 7-DHC persisted even after 72 hours, reaching the value of 86%. On the other hand, the amount of 7-DHC transformed into other derivative compounds ranged from 4 to 7%. To note that a small proportion of 7-DHC could be lost during the various steps of the procedure either for the contact with the glass and with the plastic of the containers used in the experiments. In addition, care was taken during the manipulation of cell cultures to reduce the effects of light radiations on 7-DHC. Nevertheless, we have measured the levels of the compounds derived from cholesterol and 7-DHC, and we found that at basal state the culture medium enriched with 7-DHC (38.5 μg/mL) already contained mainly three sterol derivatives (cholesta-4,6,8(14)-trien-3ol, cholesta-5,7,9(11)-trien-3ol, cholesta-5,8,24-trien-3ol) whose sum was on average accounted for 13 μg/well (less than 2 μg/mL). These compounds have been already described in the literature as derivatives of non-enzymatic transformation of 7-DHC. As described for 7-DHC, also these derivative compounds entered rapidly the cells. In addition, from GC-FID and GC-MS analyses of A2058 melanoma cell extracts we found a new metabolite, undetectable in media, identified as 25-hydroxy-7-DHC; this result was also confirmed by LC-MS/MS (Tab. 3, and Tab. 4). Moreover, at basal state, the medium enriched with 7-DHC (38.5 μg/mL) contained small amounts of 7-keto-cholesterol, 7-keto-DHC, and DHCEO, even though their total amount was less than 1 μg/mL (Tab. 4). However, the concentration of these compounds, found in 7-DHC treated cells, is likely too low to be considered toxic for cell growth [28]. Therefore, it is possible to hypothesize that 7-DHC as such, and not its oxidized derivatives, is responsible for the reduced cell proliferation observed during the treatment of melanoma cells. Hence, it

was interesting to investigate if the reduction of the cell proliferation of A2058 cells measured during 7-DHC treatment was indicative of a cell death process. The LDH activity assayed in the culture media of A2058 cells incubated up to 48 hours with 38.5 µg/mL of 7-DHC indicated a not significant release of this enzyme from cells, thus excluding a necrotic process induced by 7-DHC (Tab. 5). On the other hand, the effect of 7-DHC on A2058 cells treated for 24 hours showed an early apoptotic event detected by an increment of Annexin+/PI− cells, as well as, a late apoptotic event was revealed by an increase of PI cell incorporation after 48 hours, which became more evident after 72 hours of treatment (Fig. 4a,b). The apoptotic effect was also observed on SAN cells treated for 48 hours with 38.5 µg/mL of 7-DHC (Fig. 5). It is worth to note that during caspase dependent apoptosis PARP-1 is cleaved by caspase-3 [37]. The results obtained in A2058 7-DHC treated cells didn't show significant variation of caspase-3 activity as well as the cleavage of PARP-1 (Fig. 6). Hence, these results suggest that 7-DHC affects the viability of A2058 melanoma cell lines via an apoptotic process, which may occurs in a caspase-independent manner.

Our study indicates that 7-DHC entered rapidly A2058 cells (more than 80% after 12 hours of treatment). This influx may contribute to alter the steady state of cholesterol in the membranes of cell compartments, impairing the lipid rafts, and may contribute to trigger the production of ROS affecting the cellular redox state. The 7-DHC may also alter the permeability of mitochondrial membrane and, not least, may generate oxidized sterol derivatives [38,45]. Hence, to analyze the molecular mechanisms through which the 7-DHC exerts its cytotoxic effect in A2058 melanoma cells, we have measured the intracellular levels of ROS, GSH, and the GSH/GSSG ratio during 7-DHC treatment. The ROS production increases significantly as early as after 2 hours of incubation, and the increase is still significant up to 8 hours of treatment (Fig. 7a). In addition, 7-DHC treatment of melanoma cells impairs the intracellular redox state as demonstrated by the reduction of GSH levels and GSH/GSSG ratio after 2 hours of treatment (Fig. 7c). If melanoma cells were pre-treated with NAC as antioxidant or apocynin as inhibitor of NADPH oxidase, ROS production induced by 7-DHC was inhibited (Fig. 7b). Therefore, the modulation of ROS and GSH levels by 7-DHC treatment represents an early event that may affect cell viability. In fact, in A2058 cells pre-treated with NAC or apocynin, the apoptotic effect of 7-DHC was significantly reduced (Fig. 8). Therefore, the alteration of intracellular redox state observed during 7-DHC treatment could represent an event that contributes to modulate the cytotoxic effect of 7-

DHC on melanoma cells. Since this reduction is significant but incomplete, we believe that further investigations should be addressed to search other mechanisms involved in the cytotoxic effect of 7-DHC.

The mitochondria play a key role in activating apoptosis in mammalian cells. Mitochondrial respiratory chain is the primary source of cellular ROS, therefore, the mitochondria are the main targets of ROS detrimental effects. In particular, the major ROS target inside mitochondria is undoubtedly the permeability transition pore (PTP). In response to some pro-apoptotic stimuli the PTP assumes a high conductance that results in the dissipation of mitochondrial membrane potential (MMP), an event that triggers the mitochondria dysfunctions [39]. The reduction of mitochondrial membrane potential observed in our experiments (Fig. 9) represents a clear signal of an involvement of mitochondria in the apoptotic process during 7-DHC treatment.

Bcl-2 family proteins regulate cell death along the mitochondrial apoptosis pathway [40], playing a pivotal role in the control of MMP [46]. In particular, Bax and Bak act on mitochondria permeability, mostly at the mitochondrial outer membrane, by permeabilizing the vesicles that are composed of lipids [47]. Conversely, Bcl-2 and others anti-apoptotic Bcl-2 family members prevent the mitochondrial outer membrane permeabilization, by sequestering some pro-apoptotic proteins Bcl-2 like [47]. Hence, we analyzed the protein levels of the anti-apoptotic Bcl-2, pro-apoptotic Bax, Bcl-2/Bax ratio, as well as the cellular localization of Bax. The reduction of Bcl-2/Bax ratio, detected in A2058 melanoma cells treated with 7-DHC, resulted from an unchanged Bcl-2 levels and an increase of Bax levels detected both in cytosolic and mitochondrial fractions (Fig. 10). These data prompt us to speculate that 7-DHC, affecting both Bax levels and its mitochondrial translocation, alters the fine balance between pro-apoptotic and anti-apoptotic factors thus predisposing melanoma cells to cell death.

It is to note that the alteration of mitochondrial membrane potential can make the outer mitochondrial membrane more permeable. This causes the release of mitochondrial factors that mediate the cell death process in a caspase-dependent and/or -independent manner [47]. A significant increase of AIF, a main mediator of caspase-independent cell death [42], was found in A2058 cells incubated with 38.5 µg/mL 7-DHC for 24 hours (Fig. 11), as well as its nuclear translocation was detected by confocal analysis (Fig. 12). Hence, the rise of AIF protein level and its nuclear translocation, together with the absence of an increase of caspase-3 activity and PARP-1 cleavage, suggest that the cytotoxic effects of 7-DHC may be mainly due to a caspase-independent apoptotic process.

Therefore, if we take into account that a mix of oxysterol derivatives, coming from cholesterol and 7-DHC, were found, but their levels were very low, we suggest that the cytotoxic effect should be due mainly to the 7-DHC alone. However, much of the cytotoxicity attributable to oxysterols is due to their ability to induce apoptosis, even if there is no universal mechanism responsible for oxysterol-induced apoptosis.

Our results on the effects of 7-DHC on the melanoma cell lines could be explained by assuming that loading more sterols in cell membranes and/or changing the ratio between other-sterols/cholesterol generated a stress that induced the production of ROS, an event that alters the mitochondrial functionality. As also reported in this study, the increase of pro-apoptotic Bax protein affects the mitochondrial permeabilization, interacting with voltage-dependent anion channel/adenine nucleotide transporter, and provokes a release of some molecules, such as cytochrome c, apoptosis-inducing factor (AIF), endonuclease G, smac/DIABLO, that activate both caspase-dependent and -independent cell death pathways [48]. Other studies have documented oxysterol impacts on the balance of cellular Bax vs Bcl-2/Bcl-xL levels [45,49], but no such effect was seen in 7β-OHC-treated Caco-2 cells [50], suggesting an involvement of a Bax/Bcl-2 independent apoptotic process. These debated observations illustrate well the variability in the pathways of cell death induced by different sterols/oxysterols employed in different model systems.

In conclusion, in this study we have treated melanoma cells directly with 7-DHC in dark conditions. Furthermore, thanks to the use of an accurate and effective method to transfer the 7-DHC into the cells we have minimized the non-enzymatic oxidation of compound. Hence, this is the first report in which the biological effects found in melanoma cells are mainly attributable to 7-DHC as such. However, we believe that further studies are needed to better clarify how and where the 7-DHC acts into the cells to provoke the effects observed in this study.

5. References

[1] Kandutsch, A. A.; Russell, A. E. Preputial gland tumor sterols. 3. A metabolic pathway from lanosterol to cholesterol. J. Biol. Chem. 235:2256-2261; 1960.

[2] Bloch, K.E. Sterol structure and membrane function. CRC Crit. Rev. Biochem. 14:47-92; 1983.

[3] Herman, G. E.; Kratz, L. Disorders of sterol synthesis: beyond Smith-Lemli-Opitz syndrome. Am. J. Med. Genet. C. Semin. Med. Genet. 160C:301-321; 2012.

[4] Kelley, R. I.; Hennekam, R. C. The Smith-Lemli-Opitz syndrome. J. Med. Genet. 37:321-35; 2000.

[5] Corso, G.; Gelzo, M.; Barone, R.; Clericuzio, S.; Pianese, P.; Nappi, A.; Dello Russo, A. Sterol profiles in plasma and erythrocyte membranes in patients with Smith-Lemli-Opitz syndrome: a six-year experience. Clin. Chem. Lab. Med. 49:2039-46; 2011.

[6] Starck, L.; Lovgren, A. Diagnosis of Smith–Lemli–Opitz syndrome from stored filter paper blood specimens. Arch. Dis. Child. 82:490-492; 2000.

[7] Corso, G.; Rossi, M.; De Brasi, D.; Rossi, I.; Parenti, G.; Dello Russo, A. Effects of sample storage on 7- and 8-dehydrocholesterol concentrations analyzed on whole blood spots by gas chromatography-mass spectrometry-selected ion monitoring. J. Chromatogr. B Analyt. Technol. Biomed. Life Sci. 766:365-370; 2002.

[8] Gelzo, M.; Dello Russo, A.; Corso, G. Stability study of dehydrocholesterols in dried spot of blood from patients with Smith-Lemli-Opitz syndrome, using filter-paper treated with butylated hydroxytoluene. Clin. Chim. Acta 413:525-526; 2012.

[9] Gelzo, M.; Clericuzio, S.; Barone, R.; D'Apolito, O.; Dello Russo, A.; Corso, G. A routine method for cholesterol and 7-dehydrocholesterol analysis in dried blood spot by GC-FID to diagnose the Smith-Lemli-Opitz syndrome. J. Chromatogr. B Analyt. Technol. Biomed. Life Sci. 907:154-158; 2012.

[10] Valencia, A.; Kochevar, I. E. Ultraviolet A induces apoptosis via reactive oxygen species in a model for Smith-Lemli-Opitz syndrome. Free Radic. Biol. Med. 40:641-650; 2006.

[11] Murphy, R. C.; Johnson, K. M. Cholesterol, reactive oxygen species, and the formation of biologically active mediators. J. Biol. Chem. 283:15521-15525; 2008.

[12] Xu, L.; Davis, T. A.; Porter, N. A. Rate constants for peroxidation of polyunsaturated fatty acids and sterols in solution and in liposomes. J. Am. Chem. Soc. 131:13037-13044; 2009.

[13] Xu, L.; Korade, Z.; Porter, N. A. Oxysterols from free radical chain oxidation of 7-dehydrocholesterol: product and mechanistic studies. J. Am. Chem. Soc. 132:2222-2232; 2010.

[14] Slominski, A. T.; Kim, T. K.; Janjetovic, Z.; Tuckey, R. C.; Bieniek, R.; Yue, J.; Li, W.; Chen, J.; Nguyen, M. N.; Tang, E. K.; Miller, D.; Chen, T. C.; Holick, M. 20-hydroxyvitamin D2 is a noncalcemic analog of vitamin D with potent antiproliferative and prodifferentiation activities in normal and malignant cells. Am. J. Physiol. Cell Physiol. 300:C526-C541; 2011.

[15] Holick, M. F.; Clark, M. B. The photobiogenesis and metabolism of vitamin D. Fed. Proc. 37:2567-2574; 1978.

[16] Holick, M. F. Vitamin D: A millenium perspective. J. Cell. Biochem. 88:296-307; 2003.

[17] Holick, M. F.; Tian, X. Q.; Allen, M. Evolutionary importance for the membrane enhancement of the production of vitamin D3 in the skin of poikilothermic animals. Proc. Natl. Acad. Sci. USA 92:3124-3126; 1995.

[18] Tremezaygues, L.; Sticherling, M.; Pföhler, C.; Friedrich, M.; Meineke, V.; Seifert, M.; Tilgen, W.; Reichrath, J. Cutaneous photosynthesis of vitamin D: an evolutionary highly-conserved endocrine system that protects against environmental hazards including UV-radiation and microbial infections. Anticancer Res. 26:2743-2748; 2006.

[19] Lowe, L.; Hansen, C. M.; Senaratne, S.; Colston, K. W. Mechanisms implicated in the growth regulatory effects of vitamin D compounds in breast cancer cells. Recent Results Cancer Res. 164:99-110; 2003.

[20] Slominski, A.; Zjawiony, J.; Wortsman, J.; Semak, I.; Stewart, J.; Pisarchik, A.; Sweatman, T.; Marcos, J.; Dunbar, C.; Tuckey, R. C. A novel pathway for sequential transformation of 7-dehydrocholesterol and expression of the P450scc system in mammalian skin. Eur. J. Biochem. 271:4178-4188; 2004.

[21] Rubin, K. M.; Lawrence, D. P. Your patient with melanoma: staging, prognosis, and treatment. Oncology (Williston Park) 23:13-21; 2009.

[22] Vejux, A.; Lizard, G. Cytotoxic effects of oxysterols associated with human diseases: induction of cell death (apoptosis and/or oncosis), oxidative and inflammatory activities, and phospholipidosis. Mol. Aspects Med. 30:153-170; 2009.

[23] Moog, C.; Ji, Y. H.; Waltzinger, C.; Luu, B.; Bischoff, P. Studies on the immunological properties of oxysterols: in vivo actions of 7,25-dihydroxycholesterol upon murine peritoneal cells. Immunology 70:344-350; 1990.

[24] Schroepfer, G. J. Jr. Oxysterols: modulators of cholesterol metabolism and other processes. Physiol. Rev. 80:361-554; 2000.

[25] Brown, A. J.; Jessup, W. Oxysterols: sources, cellular storage and metabolism, and new insights into their roles in cholesterol homeostasis. Mol. Aspects Med. 30:111-122; 2009.

[26] Valencia, A.; Rajadurai, A.; Carle, A. B.; Kochevar, I. E. 7-Dehydrocholesterol enhances ultraviolet A-induced oxidative stress in keratinocytes: roles of NADPH oxidase, mitochondria, and lipid rafts. Free Radic. Biol. Med. 41:1704-1718; 2006.

[27] Korade, Z.; Kenworthy, A. K.; Mirnics, K. Molecular consequences of altered neuronal cholesterol biosynthesis. J. Neurosci. Res. 87:866-875; 2009.

[28] Korade, Z.; Xu, L.; Shelton, R.; Porter, N. A. Biological activities of 7-dehydrocholesterol-derived oxysterols: implications for Smith-Lemli-Opitz syndrome. J. Lipid Res. 51:3259-3269; 2010.

[29] Rajagopalan, N.; Lindenbaum, S. Kinetics and thermodynamics of the formation of mixed micelles of egg phosphatidylcholine and bile salts. J. Lipid Res. 25:135-147; 1984.

[30] Guan, P.; Lu, Y.; Qi, J.; Niu, M.; Lian, R.; Hu, F.; Wu, W. Enhanced oral bioavaibility of cyclosporine A by liposomes containing a bile salt. Int. J. Nanomedicine 6:965-974; 2011.

[31] Keller, R. K.; Arnold, T. P.; Fliesler, S. J. Formation of 7-dehydrocholesterol-containing membrane rafts in vitro and in vivo, with relevance to the Smith-Lemli-Opitz syndrome. J. Lipid Res. 45:347-355; 2004.

[32] Romano, S., D'Angelillo, A., Pacelli, R., Staibano, S., De Luna, E., Bisogni, R., Eskelinen, E. L., Mascolo, M., Calì, G., Arra, C., Romano, M. F. Role of FK506 binding protein 51 (FKBP51) in the control of apoptosis of irradiated melanoma cells. Cell Death Differ. 17:145e-157e; 2010.

[33] Cecere, F.; Iuliano, A.; Albano, F.; Zappelli, C.; Castellano, I.; Grimaldi, P.; Masullo, M.; De Vendittis, E.; Ruocco, M. R. Diclofenac-Induced Apoptosis in the Neuroblastoma Cell Line SH-SY5Y: Possible Involvement of the Mitochondrial Superoxide Dismutase. J. Biomed. Biotechnol. vol. 2010, Article ID 801726, 11 pages, doi:10.1155/2010/801726; 2010.

[34] Nicoletti, I.; Migliorati, G.; Pagliacci, M. C.; Grignani, F.; Riccardi, C. A rapid and simple method for measuring thymocyte apoptosis by propidium iodide staining and flow cytometry. J. Immunol. Methods 139:271-279; 1991.

[35] Bradford, M. M. A rapid and sensitive method for the quantitation of microgram quantities of protein utilizing the principle of protein-dye binding. Anal. Biochem. 72:248-254; 1976.

[36] Pulfer, M. K.; Murphy, R. C. Formation of biologically active oxysterols during ozonolysis of cholesterol present in lung surfactant. J. Biol. Chem. 279:26331-26338; 2004.

[37] Thornberry, N. A.; Lazebnik, Y. Caspases: enemies within. Science 281:1312-1316; 1998.

[38] Bakht, M. O.; London, E. Cholesterol precursors stabilize ordinary and ceramice-rich ordered lipid domain (lipid rafts) to different degrees. Implications for the Bloch hypothesis and sterol biosynthesis disorder. J. Biol. Chem. 281:21903-21913; 2006.

[39] Johnson, L. V.; Walsh, M. L.; Bockus, B. J.; Chen, L. B. Monitoring of relative mitochondrial membrane potential in living cells by fluorescence microscopy. J. Cell Biol. 88:526-535; 1981.

[40] Frenzel, A.; Grespi, F.; Chmelewskij, W.; Villunger, A. Bcl2 family proteins in carcinogenesis and the treatment of cancer. Apoptosis 14:584-596; 2009.

[41] Albano, F.; Arcucci, A.; Granato, G.; Romano, S.; Montagnani, S.; De Vendittis, E.; Ruocco, M. R. Markers of mitochondrial dysfunction during the diclofenac-induced apoptosis in melanoma cell lines. Biochimie 95: 934-945; 2013.

[42] Sevrioukova, I. F. Apoptosis-Inducing Factor: Structure, Function, and Redox Regulation. Antioxid. Redox Signal. 14:2545-2579; 2011.

[43] Lehmann, B.; Knuschke, P.; Meurer, M. UVB-induced conversion of 7-dehydrocholesterol to 1□,25-dihydroxyvitamin D3 (calcitriol) in the human keratinocyte line HaCaT. Photochem. Photobiol. 72:803-809; 2000.

[44] Reichrath, J.; Rech, M.; Moeini, M.; Meese, E.; Tilgen, W.; Seifert, M. In vitro comparison of the vitamin D endocrine system in 1,25(OH)2D3-responsive and resistant melanoma cells. Cancer Biol. Ther. 6:48-55; 2007.

[45] Olkkonen, V. M.; Beaslas, O.; Nissila, E. Oxysterols and their cellular effectors. Biomolecules 2: 76-103; 2012.

[46] Inthrani, I. R.; Tufo, G.; Pervaiz, S.; Brenner C. Recent advances in apoptosis, mitochondrial and drug resistance in cancer cells. Biochim. Biophys. Acta 1807:735-745; 2011.

[47] Green, R.; Kroemer, G. Pharmacological manipulation of cell death: clinical applications in sight? J. Clin. Invest. 15:2610-2617; 2005.

[48] Kim, R.; Emi, M.; Tanabe, K.; Murakami, S.; Uchida, Y.; Arihiro, K. Regulation and interplay of apoptotic and non-apoptotic cell death. J. Pathol. 208: 319–326; 2006.

[49] Palozza, P.; Serini, S.; Verdecchia, S.; Ameruso, M.; Trombino, S.; Picci, N.; Monego, G.; Ranelletti, F.O. Redox regulation of 7-ketocholesterol-induced apoptosis by beta-carotene in human macrophages. Free Radic. Biol. Med. 42:1579–1590; 2007.

[50] Roussi, S.; Gosse, F.; Aoude-Werner, D.; Zhang, X.; Marchioni, E.; Geoffroy, P.; Miesch, M.; Raul, F. Mitochondrial perturbation, oxidative stress and lysosomal destabilization are involved in 7beta-hydroxysitosterol and 7beta-hydroxycholesterol triggered apoptosis in human colon cancer cells. Apoptosis 12:87–96; 2007.

.

Publication list of Dr. Monica Gelzo produced during PhD course

Peer-reviewed pubblications

1. **Gelzo M**, Granato G, Albano F, Arcucci A, Dello Russo A, De Vendittis E, Ruocco MR, Corso G. Evaluation of cytotoxic effects of 7-dehydrocholesterol on melanoma cells. Free Radical Biology and Medicine 2014; 70:129-40.

2. D'Apolito O, Garofalo D, **Gelzo M**, Paris D, Melck D, Calemma R, Izzo F, Palmieri G, Castello G, Motta A, Corso G. Basic amino acids and dimethylarginines targeted metabolomics discriminates primary hepatocarcinoma from hepatic colorectal metastases. Metabolomics 2014; DOI : 10.1007/s11306-014-0641-2.

3. **Gelzo M**, Lamberti A, Spano G, Dello Russo A, Corso G, Masullo M. Sterol and steroid catabolites from cholesterol produced by the psychrophile Pseudoalteromonas haloplanktis. Journal of Mass Spectrometry 2014; submitted.

4. **Gelzo M**, Grimaldi M, Vergara A, Severino V, Chambery A, Dello Russo A, Piccioli C, Corso G, Arcari P. Comparison among binders composition in Pompeian wall painting styles from Insula Occidentalis. Chemistry Central Journal 2014; submitted.

5. **Gelzo M**, Clericuzio S, Barone R, D'Apolito O, Dello Russo A, Corso G. A routine method for cholesterol and 7-dehydrocholesterol analysis in dried blood spot by GC–FID to diagnose the Smith–Lemli–Opitz syndrome. Journal of Chromatography B 2012; 907:154-8.

6. Corso G, **Gelzo M**, Chambery A, Severino V, Di Maro A, Schiano Lomoriello F, D'Apolito O, Dello Russo A, Gargiulo P, Piccioli C, Arcari P. Characterization of pigments and ligands in a wall painting fragment from Liternum archaeological park (Italy). Journal of Separation Science 2012; 35:2986-93.

7. Corso G, **Gelzo M**, Sanges C, Chambery A, Di Maro A, Severino V, Dello Russo A, Piccioli C, Arcari P. Polar and non-polar organic binder characterization in Pompeian wall paintings: comparison to a simulated painting mimicking an "a secco" technique. Analytical and Bioanalytical Chemistry 2012;402:3011-6.

8. **Gelzo M**, Dello Russo A, Corso G. Stability study of dehydrocholesterols in dried spot of blood from patients with Smith-Lemli-Opitz syndrome, using filter-paper treated with butylated hydroxytoluene. Clinica Chimica Acta 2012;413:525-6.

9. Corso G, **Gelzo M**, Barone R, Clericuzio S, Pianese P, Nappi A, Dello Russo A. Sterol profiles in plasma and erythrocyte membranes in patients with Smith-Lemli-Opitz syndrome: a 6 years experience. Clinical Chemistry and Laboratory Medicine 2011;49:2039–46.

10. Corso G, D'Apolito O, **Gelzo M**, Paglia G, Dello Russo A. A powerful couple in the future of clinical biochemistry: the in situ analysis of Dried Blood Spot by Ambient Mass Spectrometry. Bioanalysis 2010;2(11):1883-91.

11. Paglia G, D'Apolito O, **Gelzo M**, Dello Russo A, Corso G. Direct analysis of sterols from dried plasma/blood spot by an Atmospheric Pressure Thermal Desorption Chemical Ionization Mass Spectrometry (APTDCI-MS) method for a rapid screening of Smith-Lemli-Opitz syndrome. Analyst 2010;135(4):789-96.

Journal contributions

1. Clericuzio S, **Gelzo M**, Barone R, Corso G, Dello Russo A. Nuovo metodo GC-FID per l'analisi rapida del colesterolo e del 7-DHC da spot di sangue intero su carta bibula pre-trattata con stabilizzante. 44° Congresso Nazionale SIBioC. Roma, 5-7 Novembre 2012. Biochimica Clinica 2012; 36(6)508.

2. Barone R, **Gelzo M**, Clericuzio S, Corso G, Dello Russo A. Determinazione degli steroli plasmatici ed eritrocitari di pazienti affetti da difetti della biosintesi e del metabolismo del colesterolo. 44° Congresso Nazionale SIBioC. Roma, 5-7 Novembre 2012. Biochimica Clinica 2012; 36(6)544.

3. **Gelzo M**, Marotta G, Di Taranto MD, D'Agostino MN, Gentile M, Fortunato G, Dello Russo A, Rubba P, Corso G. A case of cerebrotendinous xanthomatosis in a woman with a normal cholesterolemia. 24° Congresso Nazionale SISA, Roma, 24-27 Novembre 2010. Giornale italiano dell'Arteriosclerosi 2010; 1(0):71.

Book contributions

1. **Gelzo M**, Grimaldi M, Vergara A, Severino V, Chambery A, Dello Russo A, Piccioli C, Corso G, Arcari P. Comparison of organic binder composition among Pompeian four styles wall paintings excavated from Marcus Fabius Rufus house, pp 104-115. In: Diagnosis for the Conservation and Valorization of Cultural Heritage. Napoli, 12-13 Dicembre 2013; Ed. Ethos, ISBN 978-88-908168-0-2.

2. **Gelzo M**, Lamberti A, Spano G, Dello Russo A, Corso G, Masullo M. In vitro evaluation of products from cholesterol metabolism in the psychrophile Pseudoalteromonas haloplanktis, pp 171-172. In: 3rd MS Food Day. Trento, 9-11 Ottobre 2013; Ed. Franco Basioli, ISBN 978-88-7843-035-8.

3. Corso G, **Gelzo M**, Schiano Lomoriello F, Grimaldi M, Garofalo D, Chambery A, Di Maro A, Dello Russo A, Vanacore S, De Carolis E, Piccioli C, Arcari P. Comparison of organic binders and inorganic components between Pompeii wall paintings of the first, second and fourth styles, pp 319-326. In: Diagnosis for the Conservation and Valorization of Cultural Heritage. Napoli, 12-13 Dicembre 2012; Ed. Ethos, ISBN 978-88-908168-0-2.

4. Corso G, **Gelzo M**, Chambery A, Di Maro A, Schiano Lomoriello F, D'Apolito O, Dello Russo A, Piccioli C, Arcari P. Characterization of pigments and ligands in a wall painting fragment from Liternum escavations, pp 70-81. In: Diagnosis for the Conservation and Valorization of Cultural Heritage. Napoli, 15-16 Dicembre 2011; Ed. Nardini, ISBN 978-88-86208-69-7.

5. Corso G, **Gelzo M**, Garofalo D, Sanges C, Chambery A, Di Maro A, Dello Russo A, Parente A, Piccioli C, Arcari P. Analisi dei leganti organici nelle pitture murali di Pompei mediante spettrometria di massa tandem e gas cromatografia-spettrometria di massa, pp 337-352. In: Diagnosis for the Conservation and Valorization of Cultural Heritage. Napoli, 9-10 Dicembre 2010; Ed. De Vittoria, ISBN 978-88-86208-66-6.

Contribution to national and international conferences

1. Corso G, **Gelzo M**, Vergara A, Grimaldi M, Piccioli C, Arcari P. Pigments and binders in Pompeian four styles wall paintings. International conference, Built Heritage 2013, Monitoring Conservation Management. Milano, 18-20 November 2013.

2. Corso G, D'Apolito O, Garofalo D, la Marca G, **Gelzo M,** Dello Russo A. Intervalli di riferimento dell'acido orotico nelle urine, plasma e "dried blood spots" mediante cromatografia liquida ad interazione idrofilica accoppiata a spettrometria di massa tandem (HILIC-MS/MS). Congresso Nazionale Congiunto SIMMESN e SIMGePeD Bologna 2011, 27-29 Ottobre.

3. Paglia G, D'Apolito O, **Gelzo M**, Garofalo D, Dello Russo A, Corso G. A method for the quantification of sterols for a rapid screening of Smith-Lemli-Opitz Syndrome by Atmospheric Pressure Thermal Desorption Chemical Ionization-Mass Spectrometry (APTDCI-MS). Giornata di studio: La spettrometria di massa nello studio delle biomolecole. 26 Novembre 2010, Bari.

4. Paglia G, D'Apolito O, **Gelzo M**, Garofalo D, Dello Russo A, Corso G. A method for the quantification of sterols for a rapid screening of Smith-Lemli-Opitz Syndrome by Atmospheric Pressure Thermal Desorption Chemical Ionization-Mass Spectrometry (APTDCI-MS). Firenze, 9-10 Novembre 2010. Mass Spec Europe – P317. (Poster - pubblicato online su ePoster.net – The Online Journal of Scientific Posters: http://eposters.net/index.aspx?id=3369).